AD-A065 156 GEORGIA INST OF TECH ATLANTA DEPT OF CHEMISTRY F/G 20/5
SELECTIVE CHEMICAL PUMPING OF ELECTRONIC STATES AND FORMATION A--ETC(U)
1978 J L GOLE AFOSR-78-3515
UNCLASSIFIED AFOSR-TR-79-0102 NL

1 OF 2
AD
A065156

AFOSR-TR- 79-0102

LEVEL II

12

FINAL REPORT. 1 Sep 74-1 Oct 78.

ON

Selective Chemical Pumping of Electronic States

and

Formation and Deactivation Processes in Electronic Transition Chemically Pumped Lasers

Prepared for

114 p.

Air Force Office of Scientific Research

Grant No.'s

1978

AFOSR-78-3515

AFOSR-78-2758

Period Covered September 1, 1974 - October 1, 1978

James L. Gole

Assistant Professor
Department of Chemistry
Massachusetts Institute of Technology 02139

Associate Professor
Department of Chemistry
Georgia Institute of Technology

411084 New

Special Note

This final report summarizes research carried on by Professor James L. Gole and his research group at the Georgia Institute of Technology and the Massachusetts Institute of Technology. Funding at the Massachusetts Institute of Technology was joint with Professor J.I. Steinfeld under the title "Formation and Deactivation Processes in Electronic Transition, Chemically Pumped Lasers" (AFOSR-78-2758). Funding at the Georgia Institute of Technology was under the title "Selective Chemical Pumping of Electronic States" (AFOSR-78-3515).

Abstract

A variety of high temperature techniques are applied to the study of visible chemiluminescent phenomena over the pressure range 10^{-6} to 10^{2} torr in order to assess the applicability of several reaction systems for the development of visible chemical lasers. Efforts have focused on selective formation of excited electronic states, the nature of electronic state interactions and the behavior of these states over a wide pressure range. In studying chemiluminescent spectra, efforts have concentrated on the determination of activation energies for excited state formation, the determination of excited state quantum yields, the determination of approximate radiative lifetimes for long-lived states, the assessment of rapid energy transfer routes among excited electronic states and the analysis of collisional quenching. Promising systems have been and are being explored in an exploding wire laser system.

Table of Contents

Table of Contents (continued)

1. Introduction - Topics Covered

In the course of the following studies under Air Force sponsorship, we have been concerned with the application of a variety of high temperature techniques to the development and analysis of promising systems for visible chemical laser technology. This work has involved the orderly study of chemiluminescence phenomena from 10^{-6} to 10^{2} torr. Hence we have studied the optical phenomena characterizing chemical reaction in beams, flows and flames. We have determined the visible optical signatures for a wide variety of reactions which involve both simple metathesis

$$A + BC \rightarrow AB.. + ..C \qquad (1)$$

where A is a metal atom or complex processes

$$RA + BC \rightarrow AB + (R) + (C)... \qquad (2)$$

In reaction (1), the metal atom is usually reacted in the form of a beam or, at higher pressures, metal atoms are entrained in a carrier gas, an appropriate oxidant then being introduced into the entraining flow. In reaction (2), AB may be the product of several reaction steps. The species RA may first undergo several abstraction reactions before an oxidation to produce the species AB occurs. Hence R is written in parenthesis in reaction (2) because its exact character may not be maintained. For the majority of systems considered, the reactant RA yields a minimum of two final fluorescing products including the AB molecule of greatest interest. In general the metathesis (2) will involve two room temperature gas phase species and we refer to this as a gas-on-gas system. In contrast the metathesis (1) at low pressures is referred to as a beam-gas arrangement. In all cases the reactant BC is a rather strong oxidant such as the homo- and heteronuclear halogens, NO_2, N_2O, O_3 or ClO_2.

The inclination to study complex metatheses such as those represented by reaction (2) results wholely from an emphasis to produce the desired excited states from the initial intimate combustion of two gas phase room temperature reactants. While we will summarize these studies in the report, our efforts have concentrated primarily on excited state production via metal oxidation.

There are a few basic parameters on which one would like to focus in developing systems for visible chemical lasing. Among the most obvious are the following:

(1) One should search for systems which are characterized by selective excited state formation.

(2) Selectively formed excited states should be formed with high quantum yields (copious excited state production).

(3) The lifetimes of those excited states in which we focus interest should be on the order of 10^{-6} to 10^{-4} seconds.

This criteria is determined by the time necessary for intimate reactant mixing at typical laser operating pressures. At 6 torr the requisite mixing time is $\sim 10^{-5}$ seconds.[1] It will do no good to attempt to study lasing from systems whose lifetimes are considerably shorter or longer than the time necessary for mixing of the reactants to form a lasing medium at the pressures at which one wishes to operate.[2]

(4) Excluding collision-induced transfers among excited states at higher pressures, the criteria of selectivity and high quantum yield virtually require that the activation energy for excited state product formation be less than or equal to the activation energy for ground state product formation in a given system. Hence, one must establish the temperature coefficient for any metatheses producing the excited states of interest.

(5) In studying reactions from low ($\leq 10^{-5}$ torr) to high pressures ($\leq$ 10 torr), excited state deactivation (quenching) should be at a minimum.

(6) At higher pressures, rapid collisional transfer rates among excited electronic states, especially those involving long-lived reservoir states, must be catalogued.

A good portion of our research effort has focused on the determination of activation energies for excited state formation using a recently developed procedure for the analysis of beam-gas chemiluminescent reactions.[3,4,5,6,7] We have determined and will continue to determine quantum yields and excited state radiative lifetimes. Lifetime studies involve the application of pulsed laser techniques[8] as well as determination of approximate lifetimes through study of the pressure dependence of chemiluminescent emission.[9] We have also been concerned with the very efficient energy transfer routes connecting the excited states of high temperature molecules. These transfer routes manifest themselves as one extends "single collision" chemiluminescent studies ($\simeq 10^{-6}$ to 10^{-4} torr)[9] to higher pressures commensurate with the operation of a typical chemical laser system (1 to 100 torr). Our focus in these studies has been in large part on metal oxidation reactions and the controlled relaxation of distributions observed under single collision conditions. Finally, we have attempted to achieve lasing action in those systems which we deem promising using an exploding wire laser system developed at Los Alamos Scientific Laboratory.[10] This system was moved from Los Alamos to our laboratory and is currently being used to study Group IIIB metal-halogen systems.

2. Group IIIB Metal Oxidation - An Approach to Selective Population of Excited Electronic States

As a specific example we will discuss Group IIIB metal oxidation which serves to exemplify the nature of our approach to the chemical laser problem. A more thorough discussion can be found in the attached preprint (Appendix A) and reprint (Appendix B). The discussion of other systems will follow.

Previously,[11,12] we have outlined an approach to the selective production of excited electronic states in chemical reaction. Briefly we have chosen to look at systems in which the molecular orbital makeup of certain excited electronic product molecule states, accessible to a chosen chemical reaction, differs substantially from the ground or low-lying states of this product molecule. We ask whether this substantial change will affect the branching ratio of a chemical reaction and lead to preferential population of these excited states. In order to achieve this criteria, we focus on the oxidation of those metals whose atomic orbital makeup undergoes[13] a pronounced change upon promotion from the ground to a very "low-lying" excited electronic state. We will consider those product molecule excited states which correlate with these low-lying excited metal atoms states in dissociation. It is likely that these product states will have molecular orbital makeups differing substantially from the ground or low-lying states of the product molecule. In order to insure the possible population of these excited electronic product molecule states in a "single collision" bimolecular process, we also require that the resulting chemiluminescing product of metallic oxidation (preferably a diatomic molecule) have a substantial bond strength. Our bond strength requirement causes us to concentrate on metal oxide or halide formation. The situation which must arise under "single collision" bimolecular oxidation of a given metal is depicted in Figure 1. The metal halide or oxide product molecule excited states which can be populated under single collision conditions must lie at energies less than the energy difference ($D_o^o(MX) - D_o^o(oxidant)$). We have denoted this energy difference by a horizontal line[14] in the figure whose separation from the dissociation asymptote of the product ground state corresponds to the bond energy of that oxidant bond broken in reaction.[13]

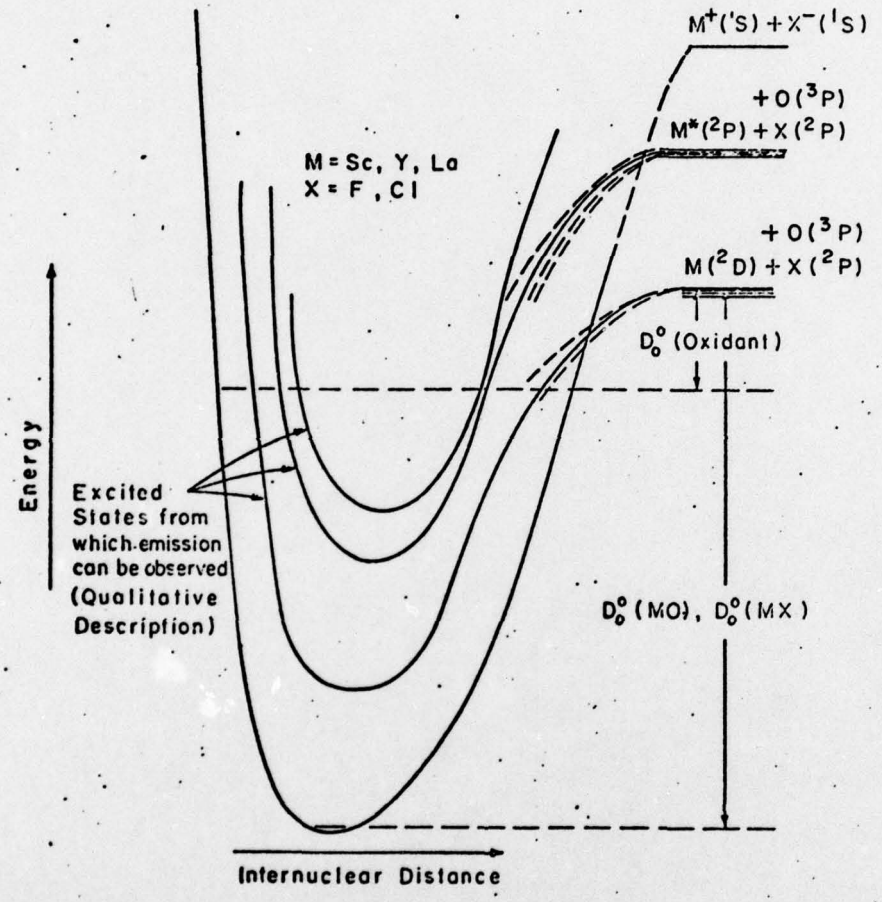
M⁺('S) + X⁻('S)
+ O(³P)
M*(²P) + X(²P)
M = Sc, Y, La
X = F, Cl
+ O(³P)
M(²D) + X(²P)
D₀° (Oxidant)
Energy
Excited States from which emission can be observed (Qualitative Description)
D₀° (MO), D₀° (MX)
Internuclear Distance

Figure 1

Our criteria are most closely fit by the metals scandium, yttrium and lanthanum. The ground states of these metals are of ^2D symmetry (electron configurations Sc, [Ar] $4s^2 3d$; Y, [Kr] $5s^2 4d$; La, [Xe] $6s^2 5d$) and all three atoms have "low-lying" ^2P electronic states (electron configuration...$s^2 p$). Here, from the standpoint of a single determinant description, we have a considerable change in atomic orbital makeup, from d to p atomic orbital character.[13] Our selection is based on single determinant arguments and does not take into account configuration interaction between atomic states. Nevertheless the ground ^2D and "low-lying" ^2P states have considerably different atomic orbital makeups. We consider those excited molecular states which dissociate to Sc*, Y* or La* (^2P). We expect that these excited molecular states will differ substantially in molecular orbital makeup from the ground and very low-lying excited states of the metal oxides or halides. A priori, it is not clear whether these states will be formed selectively in a bimolecular chemical reaction; however, this outlined approach represents a screening principle.[15]

We have characterized several Group IIIB metal reactions with the halogens, O_2, NO_2, N_2O and O_3.[11,16,17-19] Let me summarize our findings (see also Appendices A and B).

A. The Chemiluminescent Spectra (single collision beam-gas)[20]

All of the spectra resulting from reactions of each metal with the various oxidants employed have been discussed in detail.[11,16,17-19] We note here the most important trends deduced from our studies of these chemiluminescent spectra.

1. $M + RO \rightarrow MO^* + R$

We find that reactions of Group IIIB metals with oxygen-containing compounds produce the diatomic oxides MO* in relatively non-selective distributions of energetically accessible excited electronic states. As an example, the observed YO* emission from the Y-N_2O reaction is shown in Figure 2. Although these distributions do not reflect selective excited state formation, neither do they agree with predicted statistical distributions assuming no dynamical constraints.[21] The reactions of Sc and Y with O_2 are the only exception to the non-selective trend. These reactions result in predominant population of the low-lying $A'^2\Delta$ state of ScO and YO. For the Y-O_2 reaction, we have estimated that the flux into the $A'^2\Delta$ state of YO is at least 50 times that into the $A^2\Pi$ state.[18] No other electronic states are energetically accessible in the reaction.

For each metal, we also find that, as reaction exothermicity increases ((R-O) bond strength decreases), the emission intensity shifts to shorter wavelengths. This implies that the observed reactions tend to populate, at least to some extent, all energetically accessible states of the oxide.

2. $M + RX \rightarrow MX^* + R$

We have studied the chemiluminescent emission under "single collision" conditions from 19 reactions of the Group IIIB metals scandium, yttrium and lanthanum with the halogens F_2, Cl_2, Br_2, I_2, SF_6, ClF, IBr and ICl. We summarize the reactions studied in Table I. Observed chemiluminescent spectra are primarily attributed to emission from the metal monohalide formed via the reaction

$$M + RX \rightarrow MX^* + R \qquad (1)$$

YO* CHEMILUMINESCENT SPECTRUM

$Y + N_2O \longrightarrow YO^* + N_2$

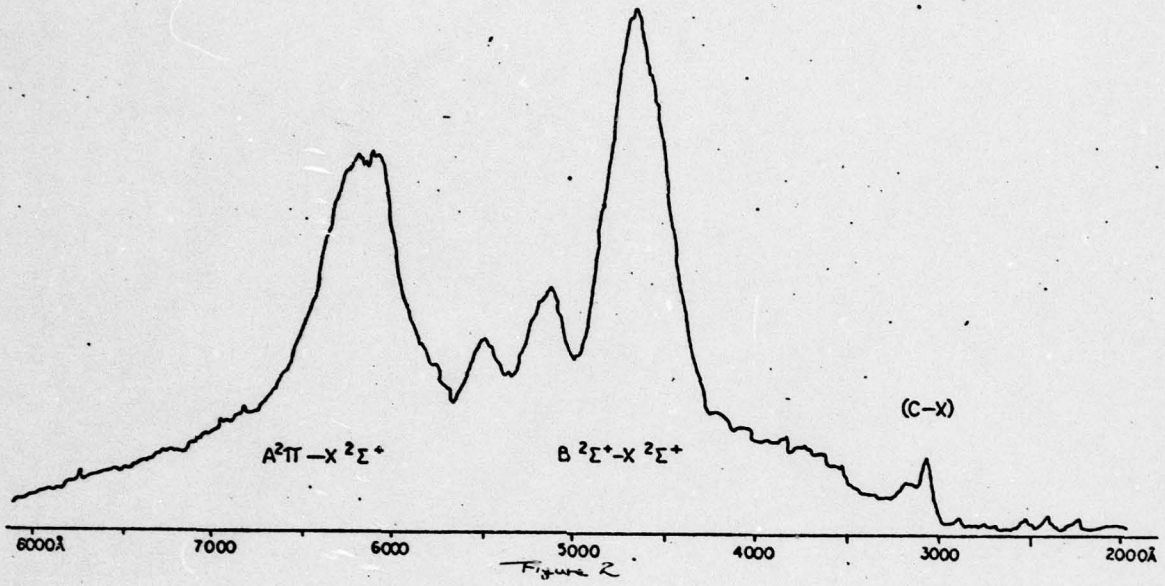

Figure 2

Table I

Group IIIB - Halogen Reactions Studied Product Formation

	Sc	Y	La
F_2	ScF^S	YF^S	LaF
Cl_2	$ScCl^2$, $ScCl_2{}^c$	YCl^S	LaCl
Br_2	$ScBr^S$, $ScBr_2{}^c$	YBr^S	---
I_2	ScI^S, $ScI_2{}^c$	YI^S	---
SF_6	ScF^S	YF^S	LaF
ClF	$ScF^S > ScCl$	$YCl^S > YF^S$	LaF, LaCl
ICl	$ScCl^S > ScI$	$YCl^S > YI^S$	---
IBr	$ScBr^S > ScI$	$YBr^S > YI^S$	---

s = selective monohalide emission

c = continuous emission due to dihalide

Dihalide emission is also observed in the Sc-Cl_2, Sc-Br_2 and Sc-I_2 systems. The dihalides appear to be formed in the reaction sequence

$$M + RX \rightarrow MX^* + R \qquad (2)$$

$$MX^* + RX \rightarrow MX_2^* + R \qquad (3)$$

We find extremely selective production of monohalide excited electronic states in both the scandium and yttrium reactions. As an example, the observed YCl* emission from the Y-Cl_2 reaction is shown in Figure 3. The lanthanum reactions are characterized by relatively moderate selective excitation of monohalide excited states. The selective feature dominating the scandium and yttrium monohalide spectra has not been observed by previous researchers. On the basis of molecular orbital theory, energy conservation, and the known spectra for scandium and yttrium fluoride, the selective emission feature is assigned to a $^3\Sigma^+ - {}^1\Sigma^+$ or $^3\Sigma^+ - {}^3\Delta$ band system.

Unlike the observed metal oxide formations, reaction exoergicity and the density of energetically accessible excited states appears to have little effect on the distribution of excited states populated. Thus, for each metal, increasing the exothermicity of the reaction by decreasing the oxidant bond strenth has little effect on the observed distribution or selectivity of populated states. As we will discuss shortly, it is possible to estimate the radiative lifetime of chemiluminescing excited states provided that these states are sufficiently long-lived so as to undergo collisions before radiating.[22] Based upon mechanistic considerations entailed in the kinetics of metastable excited states,[22] the radiative lifetimes of the selectively populated excited states of ScCl, ScBr and YCl are estimated to be on the order of 2×10^{-3} seconds. Therefore, we are

CHEMILUMINESCENT SPECTRUM

$Y + Cl_2 \longrightarrow YCl^* + Cl$

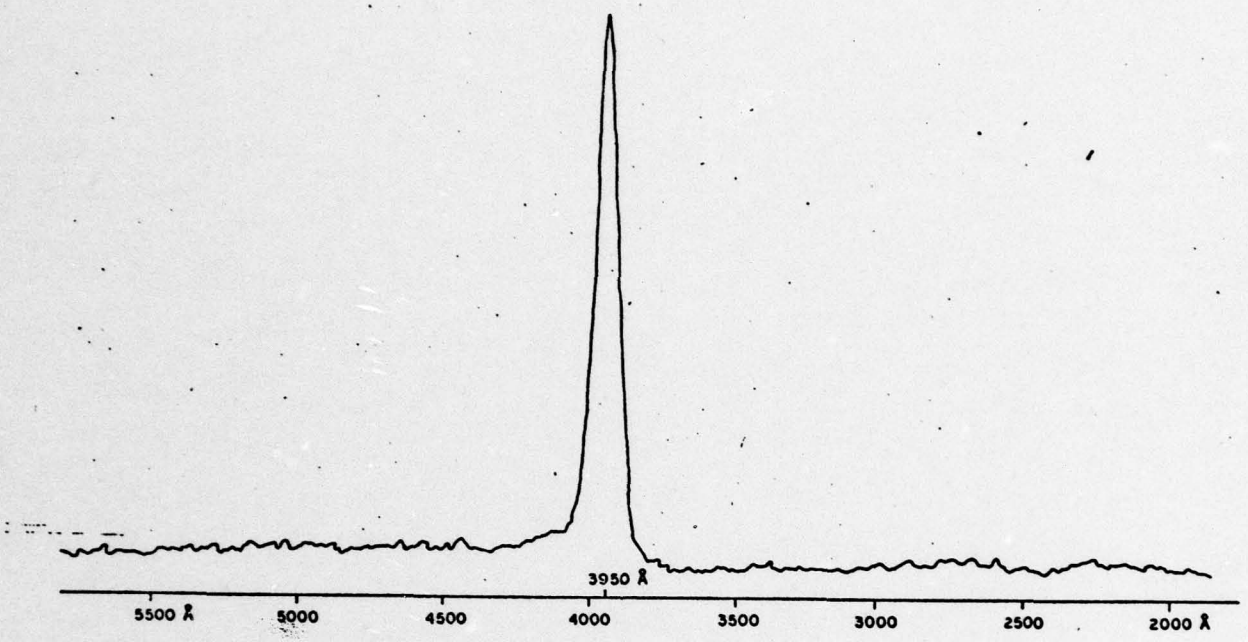

Figure 3

observing emission from moderately long-lived states. This is in contrast to the metal oxides which are characterized by much more rapid emission rates.[23]

B. Activation Energies

We have summarized measured activation energies for several reactions forming metal oxide and metal halide excited states in Tables II and III. With the exception of $YO(A'^2\Delta)$ production via the $Y-O_2$ reaction, all metal oxide forming reactions (Table II) proceed with non-negligible activation energies.[4] In contrast to those processes leading to excited state metal oxide formation, we find negligible activation energies (Table III) for formation of the $^3\Sigma^+$ metastable excited state.[11,12] As is apparent from Table III, it is not a trend characteristic of metal monohalide formation in general, but rather reflects the nature of processes corresponding to formation of specific excited states. The reaction resulting in formation of the YF C $^1\Sigma^+$ state proceeds with a substantial activation energy.[11,12] In Table III, we also present the results of our temperature dependence studies on the $Ca + F_2 \rightarrow CaF^* + F$ and $Sr + F_2 \rightarrow SrF^* + F$ reactions. Excited state formation in these reactions also proceeds with a substantial activation energy.

C. Quantum Yields[24]

The quantum yield is defined as the ratio

Excited State Emitters/Total Product Molecules Formed

In Table IV, we summarize quantum yields for several "single collision" electron transfer metal oxidations. While the quantum yields for Group IIIB oxide and Group IIA halide formation are quite small in general, being on the order of 10^{-2} to 10^{-3}%, Group IIIB halide formation

Table II

Activation Energies for Formation of ScO, YO, LaO

Reactions Studied	Activation Energy (kcals/mole)
$Sc + O_2 \rightarrow ScO^*(A^2\Pi_{1/2})$	5.13 ± 3.59
$Sc + NO_2 \rightarrow ScO^*(A^2\Pi_{1/2})$	7.85 ± 1.18
$Sc + NO_2 \rightarrow ScO^*(B^2\Sigma^+)$	6.43 ± 1.25
$Sc + N_2O \rightarrow ScO^*(A^2\Pi_{1/2})$	14.16 ± 2.44
$Y + O_2 \rightarrow YO^*(A^2\Pi_{3/2})$	1.75 ± 0.52
$Y + NO_2 \rightarrow YO^*(A^2\Pi_{3/2})$	1.10 ± 0.76
$Y + N_2O \rightarrow YO^*(A^2\Pi_{3/2})$	10.45 ± 1.23
$Y + O_2 \rightarrow YO^*(A'^2\Delta)$	≈0 ± 0.86
$La + O_2 \rightarrow LaO^*(C^2\Pi_{3/2})$	2.82 ± 1.59
$La + NO_2 \rightarrow LaO^*(C^2\Pi_{3/2})$	3.17 ± 1.78
$La + N_2O \rightarrow LaO^*(C^2\Pi_{3/2})$	2.81 ± 2.17

Table III

Activation Energies for Excited State Metal Monohalide Formation

Reactions Studied[a]	Activation Energy (kcals/mole)
$Sc + F_2 \rightarrow ScF^*(^3\Sigma^+) + F$ (selective feature at 3460 Å)	0 ± 1.8
$Sc + Cl_2 \rightarrow ScCl^*(^3\Sigma^+) + Cl$ (selective feature at 3500 Å)	1.2 ± 1.5
$Y + F_2 \rightarrow YF^*(^3\Sigma^+) + F$ (selective feature at 3800 Å)	2.0 ± 8.1
$Y + F_2 \rightarrow YF^*(C^1\Sigma^+) + F$ (emission at 5000 Å)	12.8 ± 7.0
$Y + ClF \rightarrow YF^*(^3\Sigma^+) + Cl$ (selective feature at 3800 Å)	0 ± 3.1 0 ± 6.8
$Y + ClF \rightarrow YCl^*(^3\Sigma^+) + F$ (selective feature at 3900 Å)	3.9 ± 5.1 0 ± 2.7
$Y + IBr \rightarrow YBr^*(^3\Sigma^+) + I$ (selective feature at 4040 Å)	2.4 ± 1.6
$La + F_2 \rightarrow LaF^*(^1\Pi) + F$ (prominant feature at 4730 Å)	0.8 ± 1.6
$La + F_2 \rightarrow LaF^* + F$ (short wavelength feature at 4119 Å)	4.0 ± 2.1
$Ca + F \rightarrow CaF^*(B^2\Sigma^+) + F$	3.7 ± 1.3
$Sr + F_2 \rightarrow SrF^*(B^2\Sigma^+) + F$	3.5 ± 0.8
$Sr + F_2 \rightarrow SrF^*(C^2\Pi^+) + F$	4.8 ± 1.0
$Sr + F_2 \rightarrow SrF^*(D^2\Sigma^+) + F$	4.0 ± 1.4

[a] See references 3, 4 and 12 for a discussion of activation energy determination in a beam-gas experiment.

Table IV

Quantum Yields for Electron Transfer Metal Oxidations

Reactions Studied	Quantum Yield (%)
$Sc + F_2 \rightarrow ScF^* + F$	>5%
$Y + F_2 \rightarrow YF^* + F$	>9.1%
$La + F_2 \rightarrow LaF^* + F$	>2.7%
$Sc + NO_2 \rightarrow ScO^* + NO$	1.9%
$Y + NO_2 \rightarrow YO^* + NO$	10×10^{-2}%
$La + NO_2 \rightarrow LaO^* + NO$	$\approx 20 \times 10^{-2}$%[a]
$Ba + F_2 \rightarrow BaF^* + F$	$\approx 2.1 \times 10^{-3}$%[b]
$Ca + F_2 \rightarrow CaF^* + F$	3.8×10^{-3}%

[a]Not including LaO $A'^2\Delta - X^2\Sigma^+$ emission; however, see ref. 15.

[b]Not including the BaF $A^2\Pi \leftarrow X^2\Sigma^+$ system.

proceeds with a quantum yield at least two orders of magnitude larger.

In summary, we note that Group IIIB-halogen reactions are found to proceed with unusually high "single collision" quantum yields and lead to formation of a selectively formed excited electronic state in a process characterized by a negligible activation energy. Group IIA-halogen reactions and the majority of reactions producing the group IIIB oxides are characterized by typical low "single collision" quantum yields, minimal selectivity, and substantial activation energies for excited state formation.

D. Radiative Lifetimes

Approximate Lifetimes for Long-Lived States

Recently, we have discussed the kinetics of metastable excited states formed in a beam-gas chemiluminescent reaction.[22] We define a metastable excited electronic state as being characterized by a radiative lifetime longer than 2×10^{-4} seconds. This is the time period necessary to traverse the viewing zone from which we monitor chemiluminescent emission. In order to analyze the observed pressure dependence behavior for the reactions producing long-lived states, we must consider two concepts: 1) long-lived excited state species formed in the viewing zone are predominantly lost to the detection system by virtue of the fact that they diffuse out of this region before emitting, 2) if the radiative lifetime of an excited electronic state is comparable to the inverse of the collision frequency characterizing inelastic collisions with the nascent products of reaction, one can observe "collision induced enhancement" of the fluorescence from this state. Here, the nascent vibrational-rotational distribution characterizing the excited electronic state must be collisionally deactivated

such that the total emission rate from the final rovibronic distribution detected exceeds that for the initially formed products. For a given beam-gas reaction, we determine the molecularity with respect to oxidant for all reactions studied, monitoring chemiluminescent intensity versus oxidant gas pressure. In general such plots for bimolecular processes show a linear dependence; however, the emission features attributed to long-lived states may be characterized by a linear onset followed by a faster increase in emission intensity. If collisional processes as those discussed above compete with spontaneous emission from the nascent products of reaction, one begins to observe nonlinear behavior in plots of chemiluminescent intensity versus oxidant pressure. It is also possible that collisional transfer from a long-lived reservoir state or high vibrational levels of the ground electronic state can lead to a non-linear pressure dependence; however, through relatively straightforward studies, this possibility can be demonstrated to be extremely unlikely.

Given typical inelastic cross sections for those processes which we are monitoring, it is possible to estimate excited state radiative lifetimes by noting the pressure at which nonlinear behavior is first observed. Because radiative lifetimes in the range from 10^{-4} to 10^{-2} seconds are very difficult to measure experimentally, a straightforward approximate method for their determination can be quite useful. As we have indicated previously (see also Appendix B and reference 22), this technique has been applied to the study of selectively formed Group IIIB halide excited states.[23]

The examples above characterize the girth of studies entailed in the initial analysis of promising chemical laser systems. This work is carried out under "single collision" conditions in a beam-gas environment. We have also considered the extension of low pressure studies to the high pressure

"multiple collision" regime. Here efforts have focused on collisional quenching and rapid energy transfer routes among excited states.

3. Multiple Collision Studies

In extending our flame studies to higher pressures, we are concerned with the rapid energy transfer routes connecting the excited states of high temperature molecules. As examples of this work, we summarize studies of aluminum and scandium oxidation. We should note, however, that similar studies on GeF ($A^2\Sigma^+ - X^2\Pi$) and SnF ($A^2\Sigma^+ - X^2\Pi$) are currently underway in our laboratory.

A. Rapid Energy Transfer Routes

We have analyzed the chemiluminescent emission for the reaction of aluminum with ozone over the pressure range 10^{-6} to 20 torr.[26,27,28] At lower pressures, an aluminum beam intersects a tenuous atmosphere of oxidant gas (10^{-6} to 10^{-3} torr) while at elevated pressures, the metal is entrained in a buffer gas (typically argon or helium), thus increasing the metal flux into the reaction zone as well as promoting relaxation phenomena. The observed chemiluminescent spectrum is characterized by emission from both the $B^2\Sigma^+$ and $A^2\Pi$ states of AlO. At pressures in excess of 1 torr, where collisional deactivation might be expected to lead to thermalization of nascent rotational and vibrational distributions, the measured $B^2\Sigma^+$ vibrational populations for this reaction follow a markedly non-Boltzmann distribution, exhibiting local maxima at vibrational levels v' = 6, 8, 12 and 14 (Figure 4a). This behavior is attributed to an initial chemical reaction $Al + O_3 \rightarrow AlO(A^2\Pi) + O_2$ followed by collision induced rearrangement $AlO(A^2\Pi) + Ar \rightarrow AlO(B^2\Sigma^+) + Ar$. The spin orbit interaction in AlO connects ro-vibronic levels of the $A^2\Pi$ and $B^2\Sigma^+$ states. Collisional energy transfer

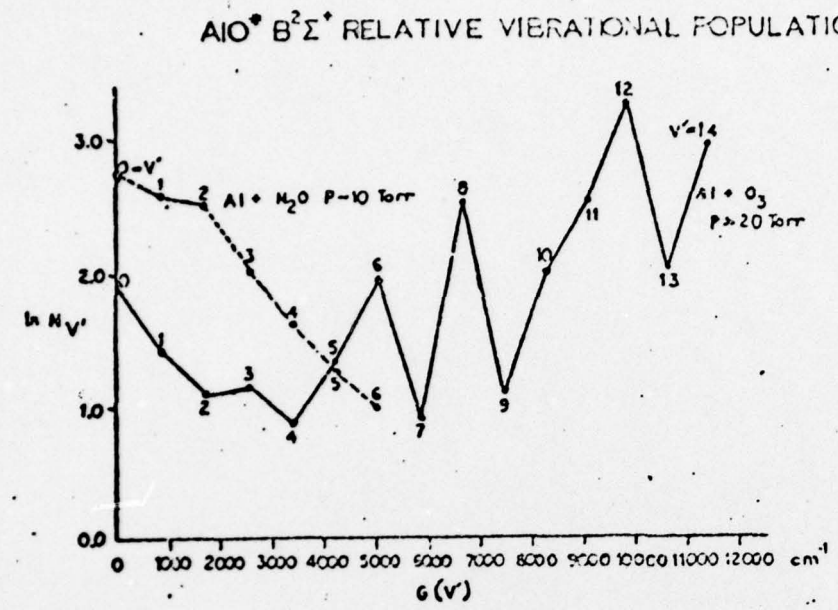

(a) $B^2\Sigma^+$ vibrational populations ($N_{v'}$) as a function of the vibrational energy term $G(v')$ for $Al + O_3$ (full line) and $Al + N_2O$ (broken line).

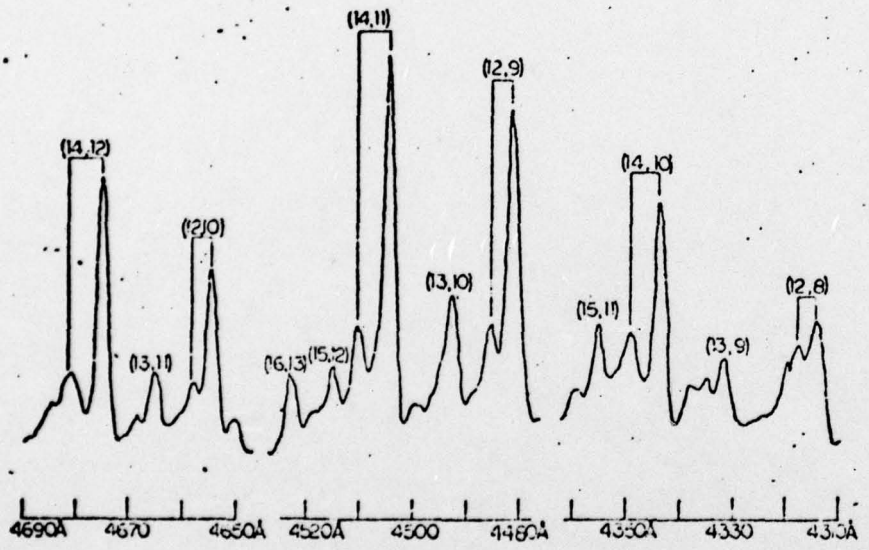

(b) Higher resolution (2 Å) scan of a portion of the $B^2\Sigma^+ - X^2\Sigma^+$ emission from $Al + O_3$. Extra bands appear as red-shifted satellites of the main (v', v'') transitions. The total (argon) pressure was 3 ½ torr.

Figure 4

is particularly efficient for the most strongly perturbed levels of the $B^2\Sigma^+$ state. In contrast, the Al + N_2O reaction is characterized by an approximate Boltzmann distribution in the AlO $B^2\Sigma^+$ state population (Figure 4a) indicating that this reaction proceeds by a different mechanism. Consistent with the proposed mechanism for Al + O_3 is the appearance of "extra" band heads representing normally Franck-Condon forbidden A-X transitions which become allowed because of a small admixture of $B^2\Sigma^+$ character. An example of these "satellite" features can be seen in Figure 4b, where the v' = 14 and v' = 12 satellites are noted. The separation between the main and satellite features is v' dependent, that is comparable for all transitions involving a given v' level. The relative intensities of the satellite and "main" transitions are strongly dependent upon argon buffer gas pressures. A quantitative description of this dependence gives an estimate for the amount of mixing between $A^2\Pi$ and $B^2\Sigma^+$ and for the rate of energy transfer between these two states. The measured rate constant for the most strongly perturbed level (v' = 14) is comparable in magnitude to the rate constant expected for hard sphere collisions between argon and AlO.

Our work on AlO has now been extended to ScO and YO. We have observed evidence for a very efficient collisional transfer among the excited states of these molecules. An example is given in Figure 5. Here we present scans of the $B^2\Sigma^+ - X^2\Sigma^+$ band system of ScO formed in the reaction of scandium with NO_2. The background pressures are 10 and 400 microns respectively (Ar added for higher pressure scans). Emission from the v' = 8 level clearly dominates the 400 micron scan and the relative intensities of the emission from the v' = 3 (3,1), v' = 8 (8,5) and v' = 13 (13,9) levels, changes drastically as the pressure is varied from 10 to 400 microns. We also note a "satellite" band appearing in the 400μ scan. This satellite corresponds to a vibrational level of a long-lived state which interacts

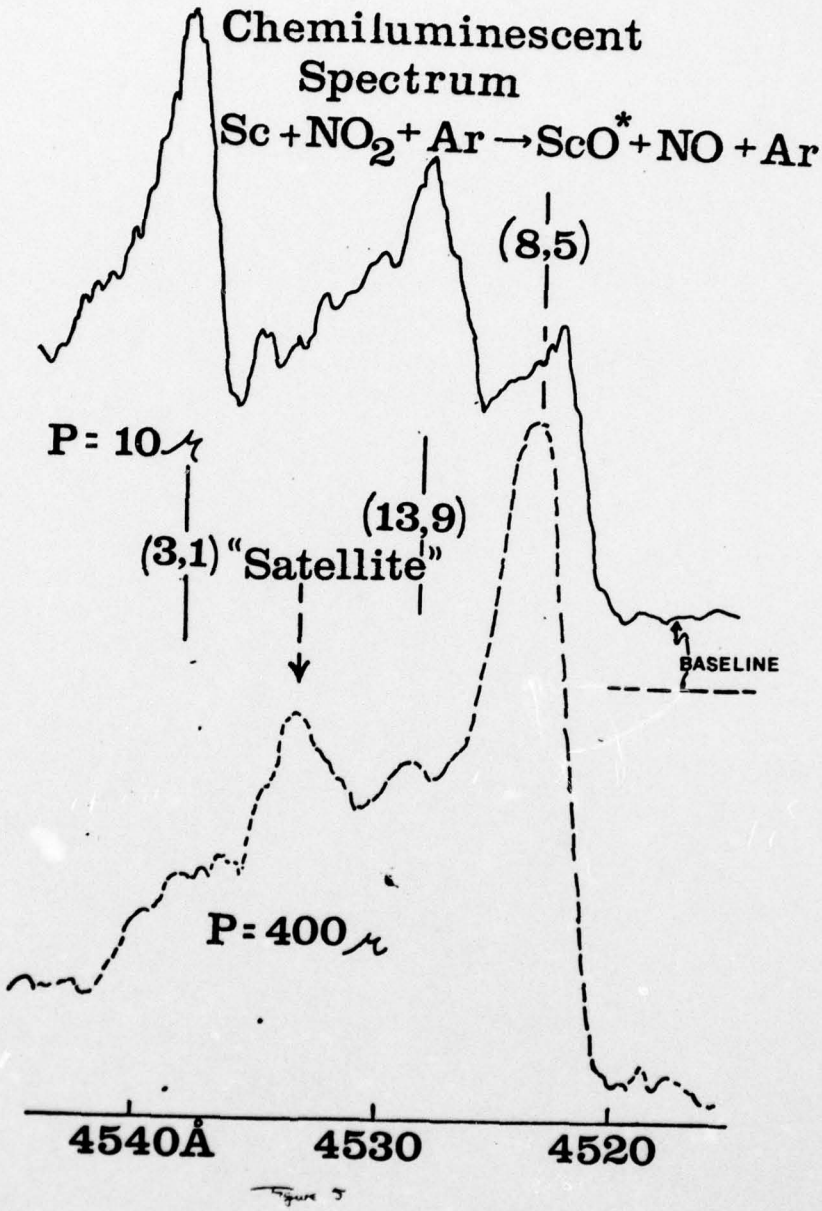
Chemiluminescent
Spectrum
Sc + NO2 + Ar → ScO* + NO + Ar
(8,5)
P = 10 μ
(13,9)
(3,1) "Satellite"
BASELINE
P = 400 μ
4540Å
4530
4520

Figure 5

strongly with the observed $B^2\Sigma^+$ state. The strong coupling results in very efficient collisional transfer to the v' = 8 level of the $B^2\Sigma^+$ state. The long-lived state borrows intensity from the $B^2\Sigma^+$ state and the transition which is nominally Franck-Condon forbidden can be observed. If we note other regions of the ScO emission spectrum, all emissions corresponding to the v' = 8 level are accompanied by a satellite band similar to that in Figure 5, and shifted an identical distance from the main feature. In these studies, we utilize the strong perturbations among the excited electronic states of high temperature molecules. Although a complete perturbation analysis of the emission spectra (all rotational levels) would be prohibitive if not impossible, the appearance of the satellite features allows us to achieve a good semiquantitative description of those "super highways" connecting these states. For the researcher interested in locating highly efficient transfer routes among excited states, this is an extremely important tool. In contrast to the ScO system, pressure dependent effects in AlO are observed in the pressure range from one to five torr. Therefore observing and analyzing these effects is not trivial. A wide variation can be found and great care and patience is required. Our preliminary work indicates that the satellite features observed in ScO (effects also observed for v' = 2, 5, 6 and 7, $B^2\Sigma^+$) correspond to rapid collisional transfer from a low-lying quartet pi state.

In order to carry out the studies which we describe, computer programs have been written to fit various transitions in experimentally observed spectra from first principles. Once an accurate fit is obtained, population distributions can be automatically extracted. Because we have the facility for independent variation of vibrational or rotational temperatures (or non-equilibrium distributions), we are able to characterize population distributions and relaxation phenomena from low pressure ($\leq 10^{-4}$

torr) single collision conditions to high pressure ($\geq$ 1 torr) multiple collision conditions.

It should be clear that, with care, these techniques can be applied to the analysis of energy transfer in a variety of potential laser candidate systems.

B. Collisional Quenching Studies

While the techniques described in the previous section are also applied to the study of collisional deactivation and quenching in these systems, we have been primarily concerned with the collisional deactivation of the selectively formed (Tables I-IV) Group IIIB halide excited states.

C. Group IIIB - Halogen Reactions at Higher Pressures

We have determined that a minimum of 10% of those product molecules formed in Group IIIB - halogen reaction are formed in an excited electronic state (reference Appendix B - Publications 13, 14). Because this is an unusually high "single collision" quantum yield, it implies a mechanism for excited state Group IIIB halide formation which differs considerably from previously studied systems (references 10-17, Appendix A - Publication 14). The magnitude of the minimum quantum yield implies possible inversions between vibrational levels of the selectively formed excited state and the ground or low-lying states to which we are observing emission. For the grid of Group IIIB - halogen reactions studied, substantial metal halide product dissociation energies and previous experimental evidence in the "multiple collision" pressure regime, imply that product molecule formation in the ground electronic state should be dominated overwhelmingly by branching into high vibrational levels. This mode of product formation may lead to possible inversions between excited state levels and the certain

vibrational levels of the ground state to which they emit. The excited state radiative lifetime, for the "selective metal monohalide feature" (reference 22 - Publications 12, 13, 2) is sufficiently long so that it slightly exceeds the critical time for intimate reactant mixing at pressures on the order of 5 torr ($\tau_m = 3 \times 10^{-5}$ p(sec.), p in torr). For this reason we have been concerned with the collisional quenching of the selective metal monohalide feature at higher pressures. We have extended our studies to the one to twenty torr pressure regime in order to assess quenching and deactivation effects. Extension to this pressure range is necessary in order that one might attain the critical inversion density necessary to achieve laser action. Initial quenching studies with argon at pressures up to 20 torr were quite promising and as a result further work with CO and CO_2 was performed. These studies have indicated minimal electronic collisional deactivation at pressures up to and acceeding 10 torr. Computer programs are now being completed to fit the observed selective $^3\Sigma^+$ spectral emission feature from single to multiple collision conditions. In addition, the current results have focused our attention on means of producing copious quantities of Group IIIB metal atoms in the vapor phase in a cavity appropriate for laser action.

D. Exploding Wire Laser

As we have noted, an exploding wire laser system has been installed in our laboratory in order to study promising laser candidates. This is a very convenient and inexpensive laboratory probe. If one is able to obtain lasing action under the pulsed conditions characterizing the exploding wire system, extension to more costly flow systems can then be undertaken. Preliminary results obtained for yttrium in a fluorine atmosphere are very

promising. We have maintained emission from the relatively long-lived selective ($^3\Sigma^+$) YF emission feature at cavity pressures in excess of 125 torr (50 torr F_2, $\geq$ 80 torr argon). We are currently undertaking a series of studies which involve higher resolution scanning of the cavity emission and coincidental system parameterization.

4. Summary of Additional Systems Studied

The previous sections have provided a fairly detailed summary of the types of studies which we have performed on a select group of molecules in order to assess their promise in visible chemical laser systems. In the following discussion we summarize the studies carried out under Air Force sponsorship on several other systems. While the molecules studied may not show promise as chemical laser candidates, the research effort has led to an increase in the data base available for several combustion processes.

A. Lanthanum Oxide Chemiluminescence

Using a beam-gas arrangement, we have studied the chemiluminescent emission which results when a thermal beam of La atoms (1750-2400K) intersects a tenuous atmosphere (10^{-6} to 10^{-4} torr) of one of the thermal oxidants O_2, NO_2, N_2O or O_3 (300K). The La-O_2 reaction is characterized by visible chemiluminescence from the $B^2\Sigma^+$ and $C^2\Pi$ states of LaO. The La-NO_2, La-N_2O and La-O_3 reactions are characterized by emission from the $B^2\Sigma^+$, $C^2\Pi$ and $D^2\Sigma^+$ states of LaO. In addition all four systems are characterized by extensive emission from the $A^2\Pi$ state of LaO. From the chemiluminescent spectrum for the La-O_2 system, a minimum value of 8.30 ± 0.04 eV is deduced for the dissociation energy of lanthanum monoxide. This lower bound is in good agreement with previous mass spectrometric determinations (8.28 ± 0.11 and 8.38 ± 0.2 eV). From the temperature dependence of the four

chemiluminescent reactions, we can elucidate the reaction dynamics of low-lying atomic states in the oxidation reactions of high temperature metallic beams (Publication 4).

Analysis of the observed chemiluminescence provides evidence for an inflection in the LaO $D^2\Sigma^+$ state for vibrational levels v' ± 8. The reflection would appear to be caused by an "avoided crossing" of two "zeroth order" $^2\Sigma^+$ states (Publication 5).

B. Scandium and Yttrium Oxide Chemiluminescence

The chemiluminescent reactions of Sc and Y atoms with O_2, NO_2, N_2O and O_3 have been studied under single-collision conditions, using a beam-gas arrangement. The reactions of Sc and Y with O_2 are characterized by emission from the $A^2\Pi$ and the previously unobserved $A'^2\Delta$ states of ScO and YO. The reactions of Sc and Y with NO_2, N_2O and O_3 result in emission from the $A^2\Pi$ and $B^2\Sigma^+$ states of ScO and YO. In addition, emission from at least one previously unobserved electronic state, lying higher in energy than the $B^2\Sigma^+$ state, is observed in the emission resulting from the Sc-O_3, Sc-N_2O, Y-O_3 and Y-N_2O reactions. From the $A^2\Pi$ - $X^2\Sigma^+$ chemiluminescent spectra for the Sc-O_2 and Y-O_2 systems, minimum values of 7.13 ± 0.1 eV for the dissociation energy of ScO, and 7.46 ± 0.1 eV for the dissociation energy of YO can be deduced. These lower bounds are in good agreement with previous mass spectrometric determinations of these quantities. Upper and lower bounds to the effective rotational temperature of ScO ($B^2\Sigma^+$, v = 0) formed in the Sc-NO_2 reaction can be determined from rotational structure observed in the B-X chemiluminescent spectrum. Measurements of the dependence of the chemiluminescent intensity on oxidant pressure and metal temperature indicate that all of the reactions studied are first order with respect to both ground state metal atom and oxidant molecule number densities. Relative rate

constants for formation of product vibrational and electronic states, determined from the chemiluminescent spectra, are found to deviate quite substantially from those predicted on the basis of prior statistical distributions obtained with no dynamical constraints (Publications 7, 16).

C. Titanium Oxide Chemiluminescence

A beam-gas arrangement has been used to study the chemiluminescent emission which results when a thermal beam of titanium atoms (2200-2650K) intersects a tenuous atmosphere (10^{-4} to 10^{-5} torr) of thermal O_2, NO_2 and N_2O molecules (300°K). The visible chemiluminescence extends from 7000 to ≃4000Å for the titanium-O_2 reaction and 700 to ≃3000Å for the titanium-NO_2 and titanium-N_2O reactions. The emission which characterizes the Ti-O_2 reaction corresponds predominantly to the $B^3\Pi$ - $X^3\Delta$ and $C^3\Delta$ - $X^3\Delta$ band systems of titanium monoxide. Some weak emission corresponding to the $c^1\phi$ - $a^1\Delta$ band system is also observed. The emission from the Ti-NO_2 and Ti-N_2O reactions is considerably more complicated; however, both reactions are characterized by strong $B^3\Pi$ -$X^3\Delta$ and $C^3\Delta$ - $X^3\Delta$ emission features. The Ti-N_2O reaction also displays strong emission from the D-$X^3\Delta$ TiO band system. Although emission is observed from the seven lowest vibrational levels of the $C^3\Delta$ state, only the emission from $0 \geq v' \geq 4$ is the result of a bimolecular process. The $v' = 5,6$ levels are formed in a process second order in oxygen molecules. From analysis of the temperature dependence of the chemiluminescent spectrum, we can determine a slope heat for the process which produces the titanium atom whose reaction with O_2 leads to the observed chemiluminescence. This slope heat is used to deduce the activation energy for the possible processes which lead to TiO $C^3\Delta$ chemiluminescence. The chemiluminescence resulting from the Ti-O_2 and Ti-N_2O reactions indicates that emission from the TiO-O_2 reaction is due

overwhelmingly to a metathesis involving excited state titanium atoms. Further analysis demonstrates that the reaction of Ti(^{5}F) excited states is the most likely process leading to the observed $C^3\Delta - X^3\Delta$ emission. From the results of temperature and pressure dependence measurements on the Ti-O_2(TiO) chemiluminescent spectrum, we deduce a lower bound of 159.8 ± 3 kcals/mole for the dissociation energy of ground state titanium monoxide. This lower bound is in close agreement with recent mass spectrometric studies. Using available spectroscopic data, we have generated an RKR potential for the first ten levels of the $C^3\Delta$ state of TiO and have deduced Franck-Condon Factors for the $C^3\Delta - X^3\Delta$ transition and estimated relative (v') vibrational level populations for the Ti-O_2 reaction (Publication 8).

D. Cerium, Dysprosium and Neodymium

The cerium, dysprosium and neodymium reactions with F_2 and NO_2 have been investigated. The chemiluminescent spectra are characterized by a broad somewhat structured emission feature extending throughout the ultraviolet and visible regions. As an example, we note the cerium-NO_2 system. The cerium-NO_2 system is characterized by a seemingly structured feature (Figure 6) extending from 3300 to 6400Å. These spectra were obtained at very low cerium flux. Work on these systems was not pursued because the density of states characterizing these metal oxides and halides was deemed too substantial to allow for sufficient population of a given excited state level. Put another way, the partition of reaction exothermicity in these systems precludes the creation of a requisite population inversion.

E. Oxidation of Silicon, Germanium and Tin

The chemiluminescence emanating from the oxidation of silicon, germanium and tin with O_3, N_2O and F_2 has been studied over the pressure

C_eO^* CHEMILUMINESCENT SPECTRUM

$C_e + NO_2 \longrightarrow C_eO^* + NO$

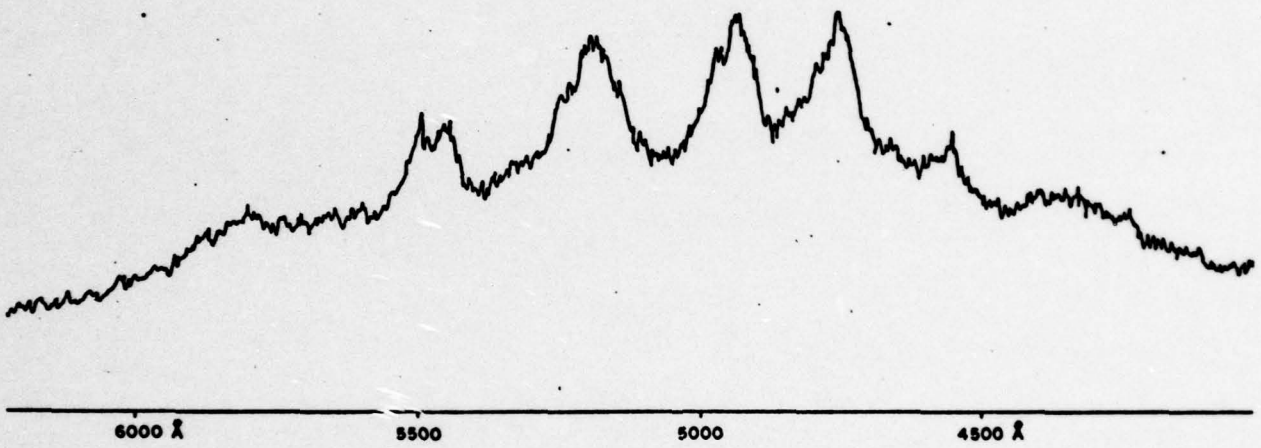

Figure 6

range from "single collision" conditions to pressures approaching 10 torr. The Si-N_2O, O_3 reactions are characterized by extensive emission from the $a^3\Sigma^+$ and $b^3\Pi$ states of SiO. A small component of SiO $A^1\Pi$ - $X^1\Sigma^+$ emission is also observed. The Ge-O_3 reaction also leads to extensive emission from the $A^1\Pi$, $a^3\Sigma^+$ and $b^3\Pi$ states. While the analysis of the "single collision" GeO spectrum is tedious due to extensive spectral overlap, the analysis of the multiple collision GeO (Ge + O_3) spectrum is almost complete and confirms our observation of these states.

The Sn-N_2O, O_3 reactions under single collision conditions are characterized by very weak (N_2O) and strong, extensive (O_3) emission from the A, B, C and D states of SnO. The observation of very weak chemiluminescence for the Sn-N_2O reaction under "single collision" conditions is consistent with the observations of other workers. The Sn-N_2O reaction is slow and is therefore not expected to yield strong chemiluminescence in a bimolecular process.

The Si-F_2, Ge-F_2 and Sn-F_2 reactions are characterized by extensive $A^2\Sigma^+$ - $X^2\Pi$ emission features. The Si-F_2 reaction is also the source of some $^4\Sigma^-$ - $X^2\Pi$ SiF emission; however, this feature is far weaker than the $A^2\Sigma^+$ - $X^2\Pi$ band system. Correcting for phototube response the ratio is 1/120 under single collision conditions. GeF may represent a more interesting candidate. While the GeF spectrum under "single collision" conditions is virtually a continuum extending from 3500 to 5200Å, the spectrum at 2 torr consists of well defined emission from the $v' = 0 \rightarrow 10$ levels of the $A^2\Sigma^+$ state. An analysis of the two torr population distribution indicates a sharp peaking at $v' = 8$. Further studies of the emission from "single" to "multiple" collision conditions indicate that this peaking may result from collisional transfer from a long-lived reservoir state characterized in a manner very much analogous to our observations in ScO and AlO.

The SnF emission spectrum is very extensive and not yet completely characterized. There are two features of greatest interest: (1) Collisional transfer effects again appear to be present as we traverse the pressure range from "single" to "multiple" collision conditions. (2) A band system which may be the analog of the $^4\Sigma^- - X^2\Pi$ system in SiF is observed.

It should be apparent that by combining our multiple collision studies with our single collision work, we are analyzing interactions and collisional transfer between excited electronic states in a manner similar to that used for AlO and ScO. This research is useful not only for the study of possible chemical laser systems but also for further general understanding of the combustion process.

5. Gas-On-Gas Systems

In an effort to assess the usefulness of gas-on-gas oxidations to produce potential excited state lasing media, we have studied several highly exothermic oxidations of the metal cluster compounds of boron and silicon. Our findings may be summarized as follow:

A. Chemiluminescent Products of Silane + Halogen Reactions

The reactions of disilane (Si_2H_6) with Cl_2, F_2 and ClF and monosilane (SiH_4) with chlorine molecules and atoms have been studied. The disilane-fluorine system is characterized by strong emission from the $A^2\Sigma^+ - X^2\Pi$ transition of SiF, the $A(^2A_1) - X(^2B_1)$ transition of SiF_2 and the $A^2\Delta - X^2\Pi$ transition of SiH. Some evidence indicates the possible observation of the $A^4\Delta - X^2\Pi$ transition in SiH. By contrast, the principal emission spectrum in the monosilane-chlorine and disilane-chlorine reactions is the $^1A'' - {}^1A'$ transition of HSiCl. A continuum emission feature may belong to $SiCl_2$ or

$SiCl_3$. The HSiCl emission intensity doubles when chlorine is reacted with pyrolyzed disilane, $Si_2H_6 \xrightarrow{\Delta} SiH_2 + SiH_4$; however, it is uneffected by the addition of chlorine atoms. Although $SiH_4 + Cl_2$ also reacts to form HSiCl* this reaction would not account for a doubling of the flame intensity. These results indicate specific chain mechanisms, which include both atomic and molecular halogens reacting with silylene molecules (SiH_2). The conclusions drawn from the chemiluminescence data are further substantiated by mass spectral analysis of the flame region (Publication 6).

B. Silane - Ozone

The promising nature of the silicon-ozone and germanium-ozone reactions which produce relatively long-lived $a^3\Sigma^+$ and $b^3\Pi$ excited state species heightened our interest in the disilane-ozone system. Here we found the complicated fluorescence to be characterized by emission from either the $a^3\Sigma^+$ or $b^3\Pi$ excited states of SiO or more likely an excited state of the previously unobserved HSiO molecule analogous to the HCO $\tilde{C}$-$\tilde{X}$ hydrocarbon flame bands.

C. Borane - Ozone and Borane - Fluorine Systems

The reactive systems $B_2H_6 + O_3$, F_2 and $B_5H_9 + O_3$, F_2 have been studied. Among the most interesting features of these systems is the specific nature of the chemiluminescence which we observe. The $B_2H_6 + O_3$ and $B_5Hg + O_3$ systems yield extensive densely spaced emission from BO_2 and minor emission from BO. The B_2H_6-F_2 and B_5Hg-F_2 systems give rise to a progression of bands due to HBF (Figure 7). The (0,0) band of the A-X band system of B-H is also observed.

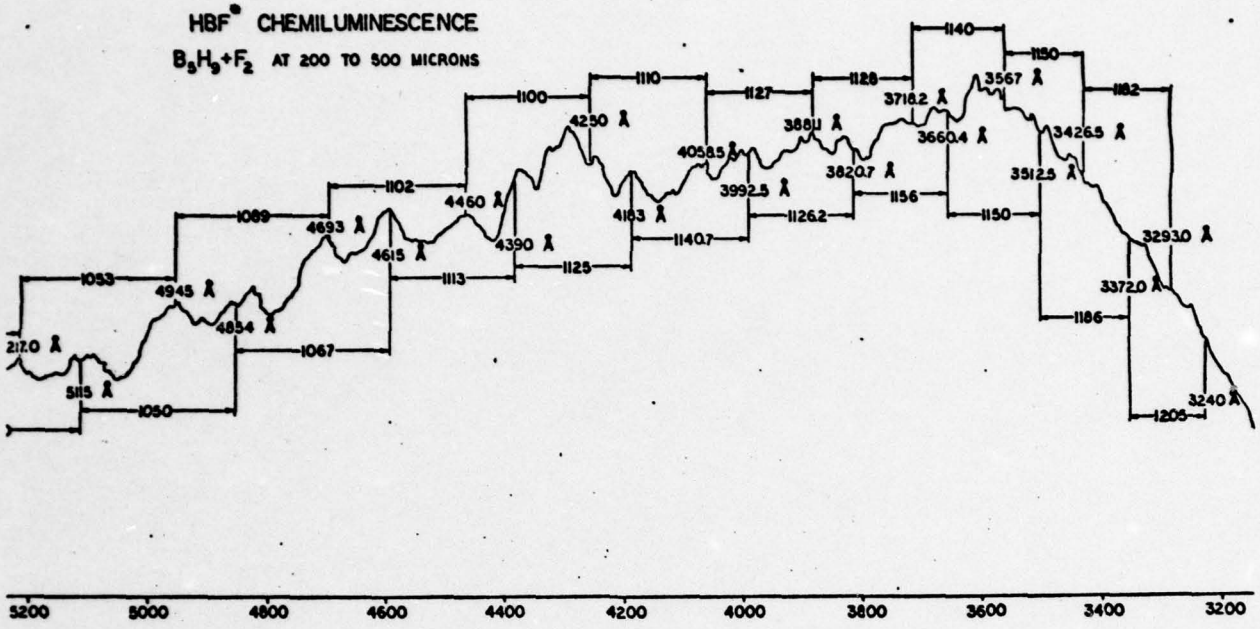
HBF* CHEMILUMINESCENCE
$B_5H_9+F_2$ AT 200 TO 500 MICRONS
1140
1150
1110
1100
1127
1128
1182
3718.2 Å
3567 Å
4250 Å
3881 Å
3660.4 Å
4058.5 Å
3426.5 Å
1102
3820.7 Å
3512.5 Å
4460 Å
3992.5 Å
1156
1089
4693 Å
4163 Å
1126.2
1150
4615 Å
4390 Å
1140.7
3293.0 Å
1053
1125
1113
4945 Å
3372.0 Å
4854 Å
1186
2170 Å
1067
5115 Å
1050
3240 Å
1205
5200
5000
4800
4600
4400
4200
4000
3800
3600
3400
3200

Figure 7

D. Chemical Laser Module

With special emphasis on gas-on-gas systems, we constructed a reaction chamber to study the possibility of obtaining visible chemical laser action or gain from highly exothermic cnemiluminescent reactions. The system was designed both as a laser cavity and as a module for extra-cavity gain studies. Initial experiments have focused on the pentaborane-fluorine system. These experiments have been slowed at present; however, they might be continued at some point in the future.

The cavity consists of two 25 cm long parallel slits of variable width down to 0.0025 cm. The slits are 0.125 cm apart, so the gas beams emanating from them cross at right angles to form a reaction zone 25 cm long and approximately 0.2 cm in diameter. The slits have been kept very narrow and closely spaced to both increase the mixing speed and confine the emission to a well defined region. The mode radius has been calculated to vary between 0.04 and 0.06 cm, depending on the position in the optical cavity. The gases are introduced into the reaction zone from long channels located behind the slits (see Figure 8). Dual inlets into each channel allow a uniform gas pressure to build up along the entire length of each slit. A carrier gas (argon or nitrogen) can be introduced into either channel to increase the effective pressure of the reactant gases. The slits can be easily cleaned of reaction byproducts by simply increasing the carrier gas pressure. The chemical laser module is also equipped with an internal cooling system capable of removing approximately 50 kcal/min.

The gas module is placed in a vacuum system ($\sim 10^{-2}$ torr) equipped with Brewster angle windows and high reflectance mirrors. The deactivated reaction products are pumped out of the chamber through four 1-1/2 inch holes in the top flange. This not only improves pumping speed, but

Schematic Diagram of Laser Cavity

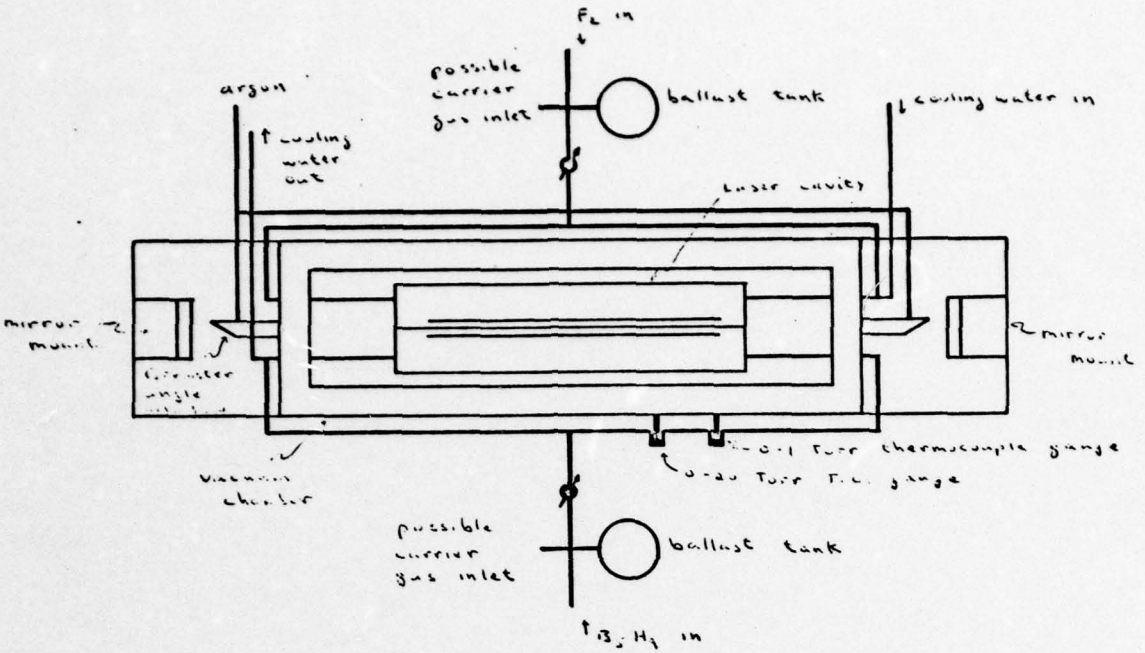

Figure 8

Cross-sectional View of Laser

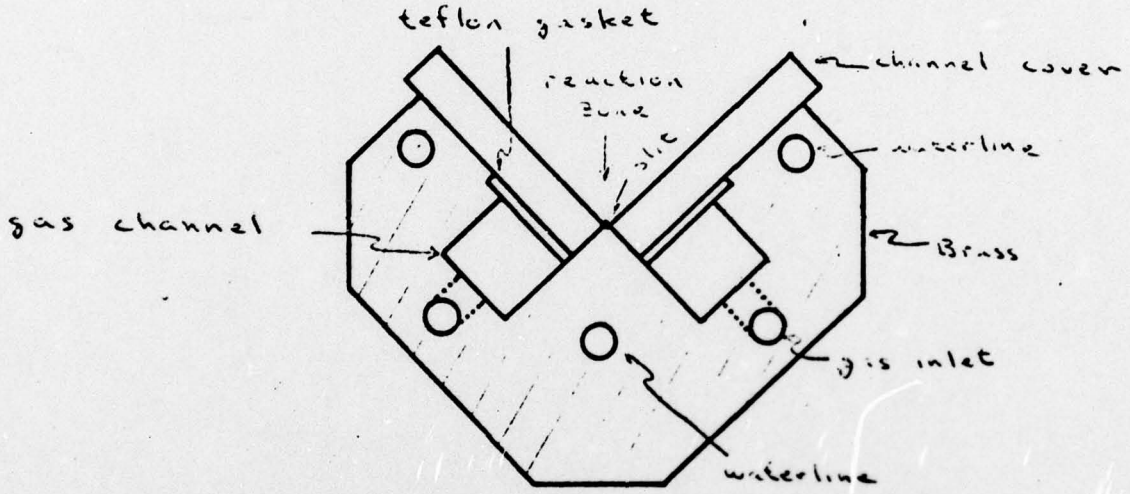

Figure 8b

decreases possible pressure gradients along the length of the cavity. The gas flows through both a fluorine trap (10 layers of 1/2 inch thick soda lime) and a particle filter before being removed from the system by a fore-pump (see Figure 9). The filters are used to protect the pump from any unreacted fluorine or particulate matter which might otherwise damage it. Two Welch 1397 vacuum pumps each remove gas at 375 liters/min; however, the gas flow is restricted by the two necessary filters. The pumping speed seems to be adequate; however, adjustments may have to be made. Typical operating pressures are in the range of 1-2 torr.

Quartz Brewster angle windows are mounted on 5 cm stainless steel tubes to minimize film formation. They are further protected from harmful oxidant gases by a blanket of argon maintained in each tube. The optical cavity is 70 cm long and is formed by a 2 meter radius of curvature concave high reflector and 0.5% transmitting flat. We can further decrease optical losses by using two 100% reflection mirrors and look at the beam scattered from one of the Brewster angle windows. With our present mirrors, we have the capability of looking at laser emission between 3500 and 6400Å.

The vacuum chamber also has six viewing ports mounted on the top flange. These can be used either for observing the reaction zone or for monitoring the spontaneous emission intensity. The optical losses due to output coupling are between 0 and 0.5% per pass. Scattering losses caused by the partial reflection from the Brewster angle windows have been decreased to approximately 0.4% per pass while the diffraction losses can be considered negligible.

Vacuum System
Vacuum chamber
top flange
fluorine trap
particle
filter
to
Welch
1397
Vacuum
Pump

Figure 1

References

1. T. Cool, private communication.
2. For short-lived states, the key to success is the ability to deactivate or alleviate the lower state to which one is emitting; that is, can you pump these molecules out of the system. For very long-lived states, requisite cavity lengths which are substantial may be prohibitive.
3. "The Temperature Dependence of Chemiluminescent Reactions - Activation Energies for Excited State Formation", Proc. Third Sum. Colloq. on Electronic Transition Lasers, Edited by Wilson, Suchard and Steinfeld, M.I.T. Press (1977), p. 176.
4. D.R. Preuss and J.L. Gole, J. Chem. Phys. 66, 2994 (1977).
5. J.L. Gole and D.R. Preuss, J. Chem. Phys. 66, 3000 (1977).
6. D.R. Preuss and J.L. Gole, J. Chem. Phys. 66, 880 (1977).
7. Carl L. Chalek and J.L. Gole, J. Chem. Phys. 65, 4384 (1976); J.L. Gole and L.H. Dubois, J. Chem. Phys. 66, 779 (1977).
8. We have available a nitrogen pumped dye laser and CMX-R4 flashlamp pumped dye laser. A nitrogen laser has been used in efforts thus far.
9. J.L. Gole, "On the Formation of the Group IIA Dihalides - Correlation of Reaction Kinetics and Molecular Electronic Structure", Chem. Phys. (submitted for publication).
10. W.W. Rice and W.H. Beattie, Chem. Phys. Lett. 19, 82-85 (1973). B.M. Dobratz, Report UCRL-51285 (Lawrence Livermore Laboratory, Sept. 1972). W.W. Rice, W.H. Beattie, J.G. Dekoker, D.B. Fradkin, Paul F. Bird and R.J. Jensen, LA-5452 (Los Alamos Scientific Laboratory, 1974).
11. "Development of Visible Chemical Lasers from Reactions Yielding Visible Chemiluminescence", James L. Gole, Proceedings of the Third Summer Colloquium on Electronic Transition Lasers, Edited by Wilson, Suchard and Steinfeld, M.I.T. Press (1977), p. 136.

12. J.L. Gole and C.L. Chalek, "Beam-Gas Chemiluminescent Reactions of Group IIIB Metals and Halogen Molecules - Evidence for Selective Excited State Emission", J. Chem. Phys., in press.

13. Here, we refer to the single determinant Hartree-Fock description of the metal atom.

14. Because of the distribution in translational energy characterizing the metal beam, this horizontal line is in reality an energy band.

15. The presence of the ionic ground state (M^+ ($...s^2$) X^- ($...p^6$)) does not affect our discussion of orbital change. If anything, it complements the desired character we seek for ground and excited states; that is a substantial change in molecular orbital character. There are many low-lying molecular states which can also correlate with the ground state neutral products (M^2D) + $X(^2P)$, and these states may effectively saturate the available d orbital character from the metal atom. Therefore we preserve our change from d to p orbital character because those states correlating with $M(^2P)$ + $X(^2P)$ will be characterized by substantial p orbital character while possessing little d orbital character from the metal atom.

16. Carl L. Chalek and J.L. Gole, Chem. Phys. 19, 59 (1977).

17. J.L. Gole and Carl L. Chalek, Proceedings of the Electrochemical Society, Electrothermics and Metallurgy, Atlanta, Georgia, 1977 (Publication 17).

18. C.L. Chalke and J.L. Gole, J. Chem. Phys. 65, 2845 (1976).

19. Note references 6 and 15.

20. A photon is emitted by the chemiluminescing species before it undergoes collision.

21. C.L. Chalek and J.L. Gole, to be published.

22. J.L. Gole, D.R. Preuss and C.L. Chalek, J. Chem. Phys. 66, 548 (1977).

23. D.M. Manos and J.M. Parson, J. Chem. Phys. 67, 1814 (1977).

24. Carl L. Chalek and J.L. Gole, "A Comparative Study of Excited State Cross Sections for Group IIIB Halide and Oxide Production - Lower Bounds for Excited State Quantum Yields" (in press).

25. See publications 9, 10, 12, 13, 14 and 17.

26. Derek M. Lindsay and J.L. Gole, J. Chem. Phys. 66, 3886 (1977).

27. M.J. Sayers and J.L. Gole, J. Chem. Phys. 67, 5442 (1977).

28. J.L. Gole and R.N. Zare, J. Chem. Phys. 57, 5331 (1972).

Personnel supported on this research grant or participating in the research carried out for the Air Force were:

Dr. Derek Lindsay

Dr. Gerald Stewart

Dr. S.A. Pace

Mr. Carl Chalek, Ph.D., September 1977

Mr. Donald Preuss

Mr. Michael Sayers

Mr. David Liu, M.S., June 1975

Mr. Larry Dubois, Currently Ph.D. program U.C. Berkeley

Mr. Steven Oblath, Currently Ph.D. program U.C. Berkeley

Mr. Winn Crumley

Mr. Gary Green

Mr. Alfred Hanner

Mr. Andrew Langford

Public Relations

Seminars and invited papers reflecting research sponsored by AFOSR were given at the following locations:

- University of Massachusetts, Boston	10/09/74
- Fifth Winter Colloquium on Quantum Electronics (Snowmass, Colorado)	02/03/75
- Cornell University	03/?9/75
- Yale University	04/14/75
- Second Summer Colloquium on Electronic Transition Lasers (Woods Hole)	09/17/75
- University of Rochester	11/22/75
- Rice University	12/22/75
- Massachusetts Institute of Technology	04/13/76 (Chemistry Department)
- Massachusetts Institute of Technology	10/15/76 (Spectroscopy - RLE Seminar)
- Third Summer Colloquium on Electronic Transition Lasers	09/08/97, 09/09/76
- University of California, Berkeley	11/09/76, 11/10/76
- University of Michigan	02/10/77
- University of Iowa	03/11/77
- Aerospace Corporation	03/15/77
- Exxon Central Research	03/30/77
- Georgia Institute of Technology	04/20/77, 04/21/77
- Electrochemical Society Meeting, Symposium on Metal Halide Chemistry	10/11/77
- Princeton University	04/10/78

- Emory University	05/23/78
- University of Toledo	06/05/78
- Gordon Research Conference on High Temperature Chemistry (invited talk)	08/07/78
- Georgia Institute of Technology	11/02/78

Cumulative List of Publications and Meeting Papers

Completed work under AFOSR-75-2758 and AFOSR 78-3515

1. C. Chalek, D.R. Preuss and J.L. Gole, "Single Collision Selective Chemical Reaction of Group III Metals (Sc, Y, La) and Halogens (F_2, ClF, SF_6 and Cl_2)", in Proceedings, 2nd Summer Colloquium on Electronic Transition Lasers (J.I. Steinfeld, ed.), p. 50, M.I.T. Press, Cambridge, MA, 1976.

*2. J.L. Gole, D.R. Preuss and C.L. Chalek, "Kinetics of Metastable Excited State Products in a Beam-Gas Chemiluminescent Reaction", J. Chem. Phys. 66, 548 (1977).

*3. D.M. Lindsay and J.L. Gole, "Al + O_3 Chemiluminescence: Perturbations and Vibrational Population Anomalies in the $B^2\Sigma^+$ State of AlO", J. Chem. Phys. 66, 3886 (1977).

*4. J.L. Gole and C.L. Chalek, "Characterization of the Ground and Excited States of Lanthanum Oxide through Bimolecular Oxidation of La Metal with O_2, NO_2, N_2O and O_3", J. Chem. Phys. 65, 4384 (1976).

5. J.L. Gole, "Correlation of Molecular Dynamics and Molecular Electronic Structure Demonstrating a Probable Inflection in the $D^2\Sigma^+$ State of Lanthanum Oxide", J. Chem. Phys., in press.

*6. C.P. Conner, G.W. Stewart, D.W. Lindsay and J.L. Gole, "Reactions of Silanes with Halogens: Chemiluminescent Products in the UV-Visible Region", J. Am. Chem. Soc. 99, 2540 (1977).

*7. C.L. Chalek and J.L. Gole, "Single Collision Chemiluminescence Studies of Scandium and Yttrium Oxidation with O_2, NO_2, N_2O and O_3", Chem. Phys. 19, 59 (1977).

*8. L.H. Dubois and J.L. Gole, "Bimolecular Single Collision Reaction of Ground and Metastable Excited States of Titanium with O_2, NO_2 and N_2O - Confirmation of $D_o(TiO)$", J. Chem. Phys. 66, 779 (1977).

9. J.L. Gole, "Development of Visible Chemical Lasers from Reactions Yielding Visible Chemiluminescence", in Proceedings, 3rd Summer Colloquium on Electronic Transition Lasers (J.I. Steinfeld, S. Suchard and L.E. Wilson, eds.), p. 136, M.I.T. Press, Cambridge, MA, 1977.

10. D.R. Preuss and J.L. Gole, "The Temperature Dependence of Chemiluminescent Reactions - Activation Energies for Excited State Formation", in Proceedings, 3rd Summer Colloquium on Electronic Transition Lasers (J.I. Steinfeld, S. Suchard and L.E. Wilson, eds.), p. 176, M.I.T. Press, Cambridge, MA, 1977.

*11. J.L. Gole, "High Temperature Chemistry: Modern Research and New Frontiers", Ann. Rev. Phys. Chem. 27, 525 (1976).

†12. "Beam-Gas Chemiluminescent Reactions of Group IIIB Metals and Halogen Molecules - Evidence for Selective Excited State Emission", with Carl L. Chalek, J. Chem. Phys. (accepted with revision).

†13. "A Comparative Study of Excited State Cross Sections for Group IIIB Halide and Oxide Production - Lower Bounds for Excited State Quantum Yields", with Carl L. Chalek, J. Chem. Phys. (accepted with revision).

†14. J.L. Gole and C.L. Chalek, "A Proposed Model for Selective Excited State Production in Electron Transfer Metal Oxidation", to be published.

15. J.L. Gole, "A Comparative Study of Group IIIB - Halogen Reactions. II. Observation of $ScCl_2$, $ScBr_2$ and ScI_2 Chemiluminescence (in preparation).

16. Burke Ritchie, C.L. Chalek and James L. Gole, "Dynamic Constraints Observed in Scandium and Yttrium Oxidation" (in preparation).

††17. "A Comparative Study of Group IIIB - Halogen Reactions. Possible Applications to Chemical Laser Development", with Carl L. Chalek, Proceedings of the Electrochemical Society, Electrothermics and Metallurgy, Atlanta, GA, 1977, Proceedings on "High Temperature Metal Halide Chemistry", Vol. 78-1, p. 278, The Electrochemical Society.

---

*Reprints and DD1473 sent.

†Preprint sent.

††Reprint enclosed (see also Appendix B).

Appendix A

A Proposed Model for Selective Excited State Production in Electron Transfer Metal Oxidations

A Proposed Model for Selective Excited State Production in Electron Transfer Metal Oxidations

James L. Gole

and

Carl L. Chalek

Department of Chemistry
Georgia Institute of Technology
Atlanta, Georgia 30332

Abstract

We present a general model for selective excited state production in electron transfer metal oxidations. This model, which represents a modification of the familiar electron jump mechanism, is formulated through comparison of several features associated with metal oxide and halide formation in beam-gas chemiluminescent systems.

Introduction

In the two preceding papers,[1,2] we have characterized several Group IIIB - halogen reactions. In the present discussion, we correlate these results with our recent studies of Group IIIB metal reactions with O_2, NO_2, N_2O, and O_3.[3-6] Through a comparison of the features associated with Group IIIB halide and oxide formation, we present a general model for selective production of excited electronic states. The model may be viewed as an extension of our previously outlined approach to selectivity.

Summary of Features Characterizing Chemiluminescing States

A. Overall Appearance of Chemiluminescent Emissions

We have summarized the general characteristics of the M + RO → MO + R and M + RX → MX + R reactions in the preceding manuscript. We simply emphasize here that those reactions yielding the metal oxides result in relatively nonselective population of excited electronic states.[4,5] The reactions of Sc and Y with O_2 are the only exception to the non-selective trend, leading predominantly to population of the low lying $A'^2\Delta$ state of ScO, and YO.[3]

In contrast, the reactions of Group IIIB metals with halogens result in formation of the diatomic halides, MX*, in moderately to highly selective distributions of excited electronic states[1]. This is not a general trend characterizing metal monohalide formation since Group IIA (Ca, Sr) metal reactions with molecular fluorine are found to lead to relatively non-selective population of excited electronic states.[6-8]

B. Activation Energies

We have summarized measured activation energies for several reactions forming metal oxide and metal halide excited states in Tables I and II. With the exception of YO ($A'^2\Delta$) production via the Y-O_2 reaction, all metal oxide forming reactions (Table I) proceed with non-negligible activation energies.[6] Many of the reactions of the Group IIIB metals with the halogens lead to selective formation of a previously unobserved long lived[1,8] $^3\Sigma^+$ excited state of the metal monohalide. In contrast to those processes leading to excited state metal oxide formation, we find negligible activation energies (Table II) for formation of this $^3\Sigma^+$ state.[1] As is apparent from Table II, this is not a trend characteristic of metal monohalide formation in general, but rather reflects the nature of processes corresponding to formation of specific excited states. The reaction resulting in formation of the YF C $^1\Sigma^+$ state proceeds with a substantial activation energy.[1] In Table II, we also present the results of our temperature dependence studies on the Ca + F_2 → CaF* + F and Sr + F_2 → SrF* + F reactions. Excited state formation in these reactions also proceeds with a substantial activation energy.

C. Quantum Yields

The quantum yield is defined as the ratio

Excited State Emitters/Total Product Molecules Formed

In Table III, we summarize quantum yields for several "single collision" electron transfer metal oxidations. While the quantum yields for Group IIIB oxide and Group IIA halide formation are quite small in general, being on the order of 10^{-2} to 10^{-3}%, Group IIIB halide formation proceeds with a quantum yield at least three orders of magnitude larger.

D. Summary

The Group IIIB- halogen reactions are found to proceed with unusually high "single collision" quantum yields and lead to formation of a selectively formed excited electronic state in a process characterized by a negligible activation energy. Group IIA- halogen reactions and the majority of reactions producing the Group IIIB oxides are characterized by typical low "single collision" quantum yields, minimal selectivity, and substantial activation energies for excited state formation.

Discussion

Electron Jump Model

We believe that the selective emission features characterizing Group IIIB-halogen reactions and the non-selective emission which characterizes formation of the Group IIIB oxides can be qualitatively explained within the framework of the familiar electron jump model.[10]

In the traditional electron jump model, reaction is initiated by a valence electron of the metal atom, M, being transferred to the oxidant molecule with which reaction takes place. Subsequent interaction of M^+ with the oxidant leads to product formation. Refinements of the electron jump model have recently been discussed by Kinsey;[11] however, we adopt the simplified picture of the electron jump mechanism. Here the covalent curve, M +(oxidant) crosses the ionic curve $M^+ + (\text{oxidant})^-$ at a distance r_c given by

$$r_c(A) = \frac{14.38}{\text{I.P.(M)} - \text{E.A.(oxidant)}} \qquad (1)$$

where I.P.(M) is the ionization potential of the metal atom, in this case scandium, yttrium,or lanthanum, and E.A. (oxidant) is the vertical electron affinity of the oxidant molecule. These energies are expressed in electron volts.

For the overwhelming number of cases, the electron jump which takes place leads to formation of the ground electronic state of that product molecule formed in reaction. One usually finds that the ionic curve corresponding to the ground electronic state of the product molecule crosses the M + (oxidant) curve at a larger internuclear distance than do those curves corresponding to any ionic excited electronic states. In most cases, this means that the electron jump mechanism will lead

predominantly to production of ground state molecules.[10,11]

The large cross sections and negligible activation energies[1] for formation of electronically excited Group IIIB halides strongly suggest that the M + RX reactions selectively populate (an) excited electronic state(s) by direct formation of MX*. In contrast, the M + RO → MO* + R reactions apparently do not proceed via this direct mechanism, but rather excited state formation occurs as a result of rearrangement from a ground state M^+ $(oxidant)^-$ complex or high vibrational levels of the product molecule ground state, both being indirect routes.[6] The difference in the magnitude of the cross section for excited state formation which characterizes the two classes of reactions may be understood in a qualitative sense upon examination of the metal-oxidant interaction potentials and the molecular electronic potential curves characterizing the metal oxide or metal halide molecule which is formed.

A Schematic Model

In this section we will describe techniques used in generating sections of the hypersurfaces characterizing the reactions of the Group IIIB metals with the halogens and the oxidants O_2, NO_2, and O_3.[12] We will first summarize our approach, presenting a schematic model which characterizes the Group IIIB halogen reactions. Following this general discussion, we will present specific examples which have lead us to the general model proposed.

Employing available spectral data for the Group III halides and oxides and generating potential curves using the technique of Padé approximants,[13] we distinguish two distinct situations. They are represented schematically

in Figures 1 and 2. These two "limiting cases" correspond to two superimposed planes of the reaction hypersurface. The selective M + X_2 reactions are characterized by an electron jump crossing radius, r_c, at a considerably smaller internuclear distance than the outer turning point of the ground state potential. The electron jump occurs at an internuclear distance such that direct transfer into the ground electronic state of the product monohalide is either negligible or is such that a strong competition for formation of ionic excited electronic states also exists. Inotherwords, direct excited state formation is facilitated. In contrast Figure 2 corresponds to a relatively non-selective reaction involving the production of a metal oxide. Here the electron jump takes place at sufficiently large internuclear distance versus the location of the metal oxide potential curves that formation of the ionic ground state is favored. In summary, selective reactions are characterized by an electron jump to (the) excited state(s) while non-selective reactions involve the traditional jump to the ground ionic state. One might envision the selective process as a "scoop" mechanism whereby the ionic excited electronic states are effectively the first ionic states to which the $M^{\oplus}$(oxidant)$^{\ominus}$ complex is exposed during the course of reaction. We believe that the selectivity and high quantum yields for the Group III-halogen reactions are due primarily to the nature of the electron jump process and secondly to the SP molecular orbital makeup of those states formed selectively. We must note that the magnitude of the selectivity which is apparent from the spectral scans in reference 1 is probably underestimated because of the long radiative lifetime characterizing the selectively formed $^3\Sigma^+$ excited state.[2] A confirmation of this point must await the direct measurement of a radiative lifetime for both selective and non-selective features and hence a comparison of relative decay rates across the observation region.

A reaction which proceeds directly via the typical electron jump mechanism is expected to be dominated by coulombic forces and to take place with little or no activation energy. Reactions proceeding indirectly or reactions which are strongly influenced by covalent forces are expected to display non-negligible activation energies.[6] In parallel with trends observed in ion-molecule reactions, one expects that reactions strongly influenced by covalent overlap will display larger barriers to reaction and, therefore larger activation energies. In view of these facts, our proposed model for selectivity is in agreement with the measured activation energies presented in Tables I and II. We find negligible activation energies for formation in the $^3\Sigma^+$ state of the metal monohalide indicating that a direct electron jump process leads to population of this particular excited state. The results presented for the Y-F_2 reaction are particularly striking because the spectral features monitored at 5000Å ($C^1\Sigma^+ - X^1\Sigma^+$ emission- Figure 3- ref. 1) correspond to emission from an excited electronic state formed with substantial activation energy in distinct contrast to the selective feature at 3800Å. This implies that the $C^1\Sigma^+$ state of YF is formed via an indirect process.[6]

Specific Examples

In Figures 3,4,5, and 6, we present, schematically, approximate interaction potentials for several M-X_2 (M = Sc, Y; X_2 = F_2, Cl_2) systems. The dashed lines represent the long range interaction between a metal atom and a halogen molecule. The M-X_2 separation r_{MX_2} corresponds to the distance between the metal atom and the nearest halogen atom. On an M-X_2 hypersurface, these curves correspond to $r_{x-x} \simeq$ constant $\simeq r_e(X_2)$. The solid curves correspond apprxoimately to the potential energy for the

MX $X^1\Sigma^+$ ground state, with $r_{X-X} \to \infty$. These MX curves were generated using [2,2] Padé approximants[13] with known MX constants.[14] The ionic curves were constructed so as to cross the neutral $M-X_2$ interaction potentials (r^{-6} potential) at the value of r_c given by equation (1), and to approach the $M^+ + X_2^-$ energy at $r_{M-X_2} \to \infty$. Generally, the vertical electron affinity is used in equation (1); however, no precise information is yet available on halogen molecule vertical electron affinities. Rather we have values for the adiabatic electron affinity which represents an upper bound to the vertical electron affinity. There are two ionic curves represented in each figure. They correspond to the adiabatic electron affinity (E.A.(F_2) = 3.08 eV, E.A.(Cl_2) = 2.38 eV)[15] and to the minimum possible vertical electron affinity (E.A.(F_2) = 1.83 eV, E.A.(Cl_2) = 1.13 eV).[16] The minimum values are equal to the difference between the electron affinity of the halogen atom and the dissociation energy of the neutral halogen molecule, X_2, which is simply the separation between the X_2 ground state potential minimum and the X_2^- dissociation asymptote. It is clear that the two coulombic curves constructed in this manner bracket the actual coulombic $M^+ + X_2^-$ curve for the system. We have also considered whether it is appropriate to represent the coulombic curves by the expression

$$\Delta E(R) = Ae^{-aR} - \frac{e^2}{R} + E(\infty)$$

where the first term corresponds to repulsive overlap of the M^+ and X_2^- ions and find that the repulsive contribution to the constructed potential is negligible for those internuclear distances comparable to or larger than r_c. Hence the coulombic curves are of the form

$$\Delta E(R) = - \frac{e^2}{R} + E(\infty)$$

where $E(\infty)$ = I.P. (Metal) - $E.A._v(X_2)$, the difference between the metal ionization potential and the vertical electron affinity of the oxidant. Similar considerations apply to the M-X_2 interaction at internuclear distances greater than or equal to r_c where repulsive overlap is certainly negligible. The zero of energy in each figure is taken as the minimum of the $X^1\Sigma^+$ potential curve.

A metal atom and X_2 molecule approach each other along the M + X_2 potential curve. At $r_{M-X_2} \sim r_c$ an electron jump from the metal atom to the X_2 molecule forms $M^+ + X_2^-$. Because of large nuclear repulsion, the X_2^- molecule dissociates, the neutral halogen atom leaving the reaction zone almost immediately.[10] Thus we have a sudden large increase in r_{X-X} corresponding to a "jump" from the dashed line curves to the solid M-X curve. One is effectively moving through a series of planes (perpendicular to the r_{X-X} axis) in the three dimensional hypersurface. The region over which the jump occurs, in terms of r_{M-X}, appears to be the key factor which determines the degree of branching into excited states of the metal halide, and hence the cross section for excited state formation. If we inspect figures 3,4,5, and 6, we find that this region varies from well outside of the ground state YF potential energy curve (Y-F_2 system - Figure 5), to well inside of the ScCl and YCl ground state curves (Sc-Cl_2- Figure 4 and Y-Cl_2 - Figure 6). This shift in the region of the jump parallels the trend in the selectivity for excited state formation in these reactions.[1] The Y + F_2 reaction is the least selective. Here the possible region for the electron jump extends from well outside to just inside of the YF ground state curve. For the Sc + F_2 reaction, which is substantially more selective, the jump region (Figure 3) extends from just outside to just inside of the ScF ground state curve. In the

case of the Sc + Cl_2 and Y + Cl_2 reactions, the jump region extends well within the outer turning points of the metal chloride ground state curve. These reactions both exhibit a very high degree of selectivity. We have not presented the analogous potential energy curves for the La-X_2 systems because the vibrational and rotational constants which characterize the LaX ground state potential are not known to sufficient accuracy so as to employ the Padé expansion. However, the La-F_2 and La-Cl_2 electron jump radii are significantly larger than those for the scandium and yttrium halide systems. Hence, one might expect that the range of possible La-X_2 jump regions paralles that found for the Y-F_2 system. This is in reasonable agreement with the observed limited selectivity for the La-X_2 reactions,[1] but we must stress that there does appear to be moderate selectivity in these systems. Excited sate formation appears to be competing significantly with ground state formation.

In Figure 7 we present an analogous set of curves which describe approximately the Sc-NO_2 system. Here we consider the location of the first ionic-covalent crossing in this system. This crossing point is determined using the vertical electron affinity of NO_2.[17] The major difference to note between the M-X_2 and Sc-NO_2 systems is the fact that the relative location of the electron jump crossing region differs quite markedly. While all of the M-X_2 systems are characterized by an electron jump region which extends to well within the MX ground state potential energy cruve, the initial Sc-NO_2 crossing point is well outside of the ScO ground state curve. We expect that further electron transfer will lead to formation of primarily ground state ScO. The population of ScO excited states occurs through an indirect route. The general makeup of other Group IIIB metal oxide systems is quite similar to that illustrated in Figure 7.[12]

We have considered the analogous planes in the hypersurfaces for the Ca-F_2 and Sr-F_2 reactions. Here, we find that the electron jump crossing region, lies at considerably larger internuclear distance than the ground state CaF and SrF potentials.

As a final point, it is important to note that the features which we have outlined for several reactions producing the metal halide and metal oxide bear little correlation with reaction exoergicity.[18] Rather, we find a strong correlation between the observed features, the relative locations of the electron jump crossing radius, r_c, and the location of the ground and excited state product molecule potentials.

The above discussion is, of course, a simplfied description of the dynamics of these reactions. To precisely describe the reactions, the three dimensional hypersurfaces for the ground and excited states of the reacting species would have to be constructed. However, since very little is known about the electronic structures of the M-RO and M-RX systems, construction of such surfaces is not possible at this time. Nevertheless we believe that the features described above and the differences which we have noted do provide a reasonable explanation for the excited stae selectivity and quantum yield results presented.

References

1. James L. Gole and Carl L. Chalek, "A Comparative Study of Group III-Halogen Reactions - Observation of a New, Selectively Populated, Excited Electronic State" J. Chem. Phys. - preceding paper.
2. Carl L. Chalek and James L. Gole, "A Comparative Study of Excited State Cross Sections for Group IIIB Halide and Oxide Production - Lower Bounds for Excited State Quantum Yields" - preceding paper.
3. Carl L. Chalek and James L. Gole, J. Chem. Phys. 65, 2845 (1976).
4. Carl L. Chalek and James L. Gole, Chemical Physics 19, 59 (1977).
5. James L. Gole and Carl L. Chalek, J. Chem. Phys. 65, 4384 (1976).
6. a) D.R. Preuss and James L. Gole, J. Chem. Phys. 66, 2994 (1977).
   b) James L. Gole and D.R. Preuss, J. Chem. Phys. 66, 3000 (1977).
7. James L. Gole, to be published.
8. J.L. Gole, D.R. Preuss, and C.L. Chalek, J. Chem. Phys. 66, 548 (1977).
9. It may be that the $^1\Pi$ - $^1\Sigma^+$ transition (Hund's case (a) or (b)) corresponds to an $\Omega = 1$ to $\Omega = 0$ transition in Hunds Case (c). If this is the case, the LaF emission feature is the analog of a $^3\Sigma^+$ - $^1\Sigma^+$ transition in the scandium and yttrium halides.
10. D.R. Herschbach, Adv. Chem. Phys. 10, 319 (1966).
11. J.L. Kinsey, "Molecular Beam Reactions" in "Biennial Reviews of Science, Technology, and Medicine, Reaction Kinetics Volume 9," Chapter 6.
12. The electron jump model is not applicable to N_2O reactions. These reactions are discussed in reference 6.
13. K.D. Jordan, J.L. Kinsey, and R. Silbey, J. Chem. Phys. 61, 911 (1974).
14. R.F. Barrow, M.W. Bastin, D.L.G. Moore, and C.J. Pott, Nature, 215, 1072 (1967).

15. W.A. Chupka, J. Berkowitz, and D. Gutman, J. Chem. Phys. 55, 2724 (1971).

16. In order to obtain these values, we have used $D_0^o(F_2)$ and $D_0^o(Cl_2)$ from A.G. Gaydon, Dissociation Energies and Spectra of Diatomic Molecules, 3rd edition Chapman and Hall, London, 1968. The electron affinities of the fluorine and chlorine atoms are from R.S. Berry and C.W. Reimann, J. Chem. Phys. 38, 1540 (1963).

17. E. Herbst, T.A. Patterson, and W.C. Lineberger, J. Chem. Phys. 61, 1300 (1974).

TABLE I

Activation Energies for Formation of ScO, YO, LaO

Reactions Studied	Activation Energy (kcals/mole)
$Sc + O_2 \rightarrow ScO^*(A^2\Pi_{1/2})$	5.13 ± 3.59
$Sc + NO_2 \rightarrow ScO^*(A^2\Pi_{1/2})$	7.85 ± 1.18
$Sc + NO_2 \rightarrow ScO^*(B^2\Sigma^+)$	6.43 ± 1.25
$Sc + N_2O \rightarrow ScO^*(A^2\Pi_{1/2})$	14.16 ± 2.44
$Y + O_2 \rightarrow YO^*(A^2\Pi_{3/2})$	1.75 ± 0.52
$Y + NO_2 \rightarrow YO^*(A^2\Pi_{3/2})$	1.10 ± 0.76
$Y + N_2O \rightarrow YO^*(A^2\Pi_{3/2})$	10.45 ± 1.23
$Y + O_2 \rightarrow YO^*(A'^2\Delta)$	$\approx 0 \pm 0.86$
$La + O_2 \rightarrow LaO^*(C^2\Pi_{3/2})$	2.82 ± 1.59
$La + NO_2 \rightarrow LaO^*(C^2\Pi_{3/2})$	3.17 ± 1.78
$La + N_2O \rightarrow LaO^*(C^2\Pi_{3/2})$	2.81 ± 2.17

TABLE II

Activation Energies for Excited State Metal Monohalide Formation

Reactions Studied[a]	Activation Energy (kcals/mole)
$Sc + F_2 \rightarrow ScF^*(^3\Sigma^+) + F$ (selective feature at 3460Å)	0 ± 1.8
$Sc + Cl_2 \rightarrow ScCl^*(^3\Sigma^+) + Cl$ (selective feature at 3500Å)	1.2 ± 1.5
$Y + F_2 \rightarrow YF^*(^3\Sigma^+) + F$ (selective feature at 3800Å)	2.0 ± 8.1
$Y + F_2 \rightarrow YF^*(C^1\Sigma^+) + F$ (emission at 5000Å)	12.8 ± 7.0
$Y + ClF \rightarrow YF^*(^3\Sigma^+) + Cl$ (selective feature at 3800Å)	0 ± 3.1 0 ± 6.8
$Y + ClF \rightarrow YCl^*(^3\Sigma^+) + F$ (selective feature at 3900Å)	3.9 ± 5.1 0 ± 2.7
$Y + IBr \rightarrow YBr^*(^3\Sigma^+) + I$ (selective feature at 4040Å)	2.4 ± 1.6
$La + F_2 \rightarrow LaF^*(^1\Pi) + F$ (prominant feature at 4730Å)[b]	0.8 ± 1.6
$La + F_2 \rightarrow LaF^* + F$ (short wavelength feature at 4119Å)	4.0 ± 2.1
$Ca + F_2 \rightarrow CaF^*(B^2\Sigma^+) + F$	3.7 ± 1.3
$Sr + F_2 \rightarrow SrF^*(B^2\Sigma^+) + F$	3.5 ± 0.8
$Sr + F_2 \rightarrow SrF^*(C^2\Pi) + F$	4.8 ± 1.0
$Sr + F_2 \rightarrow SrF^*(D^2\Sigma^+) + F$	4.0 ± 1.4

a. See reference 1 and 6 for a discussion of activation energy determination in a beam-gas experiment

b. See reference 9

Figure Captions

Figure 1. Qualitative description of potential energy curves and interactions for selective excited state formation.

Figure 2. Qualitative description of potential energy curves and interactions for non-selective excited state formation.

Figure 3. Approximate potential energy curves for the Sc-F_2 system. Curve 1 represents the coulombic potential between Sc^+ and F_2^- assuming a vertical electron affinity for F_2 of 3.08 eV. Curve 2 corresponds to a minimum F_2 vertical electron affinity of 1.83 eV. See text for discussion.

Figure 4. Approximate potential energy curves for Sc-Cl_2 system. Curve 1 represents the coulombic potential between Sc^+ and Cl_2^- assuming a Cl_2 vertical electron affinity of 2.38 eV. Curve 2 corresponds to a Cl_2 vertical electron affinity of 1.13 eV. See text for discussion.

Figure 5. Approximate potential energy curves for the Y-F_2 system. Curves 1 and 2 are analogous to those in Fig. 1. See text for discussion.

Figure 6. Approximate potential energy curves for the Y-Cl_2 system. Curves 1 and 2 are analogous to those in Fig. 2. See text for discussion.

Figure 7. Approximate potential energy curves for the Sc-NO_2 system. See text for discussion.

Figure 1

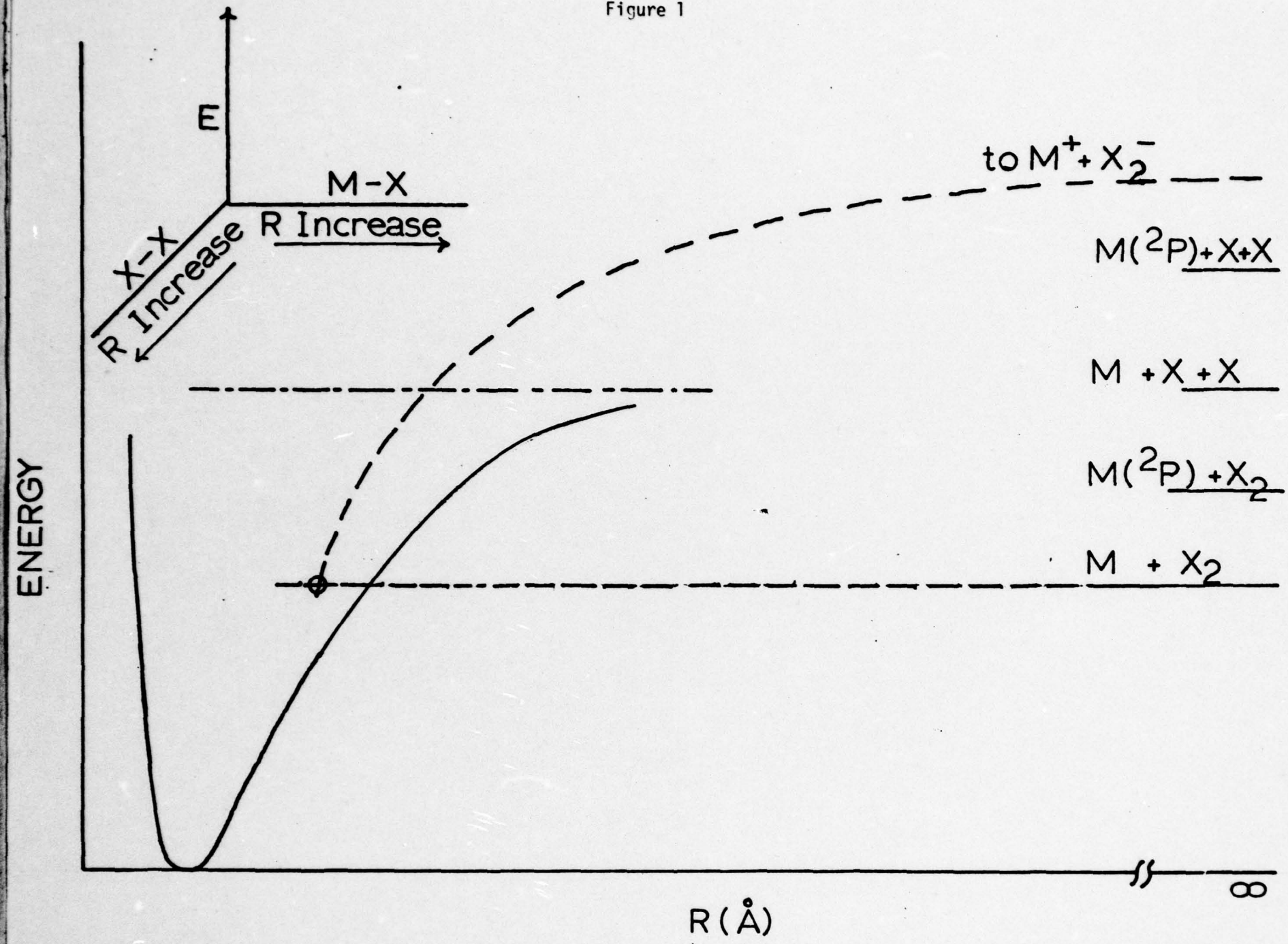
E
M-X
R Increase
X-X
R Increase
to $M^+ + X_2^-$
$M(^2P) + X + X$
M + X + X
$M(^2P) + X_2$
M + X_2
ENERGY
R(Å)
∞

Figure 2

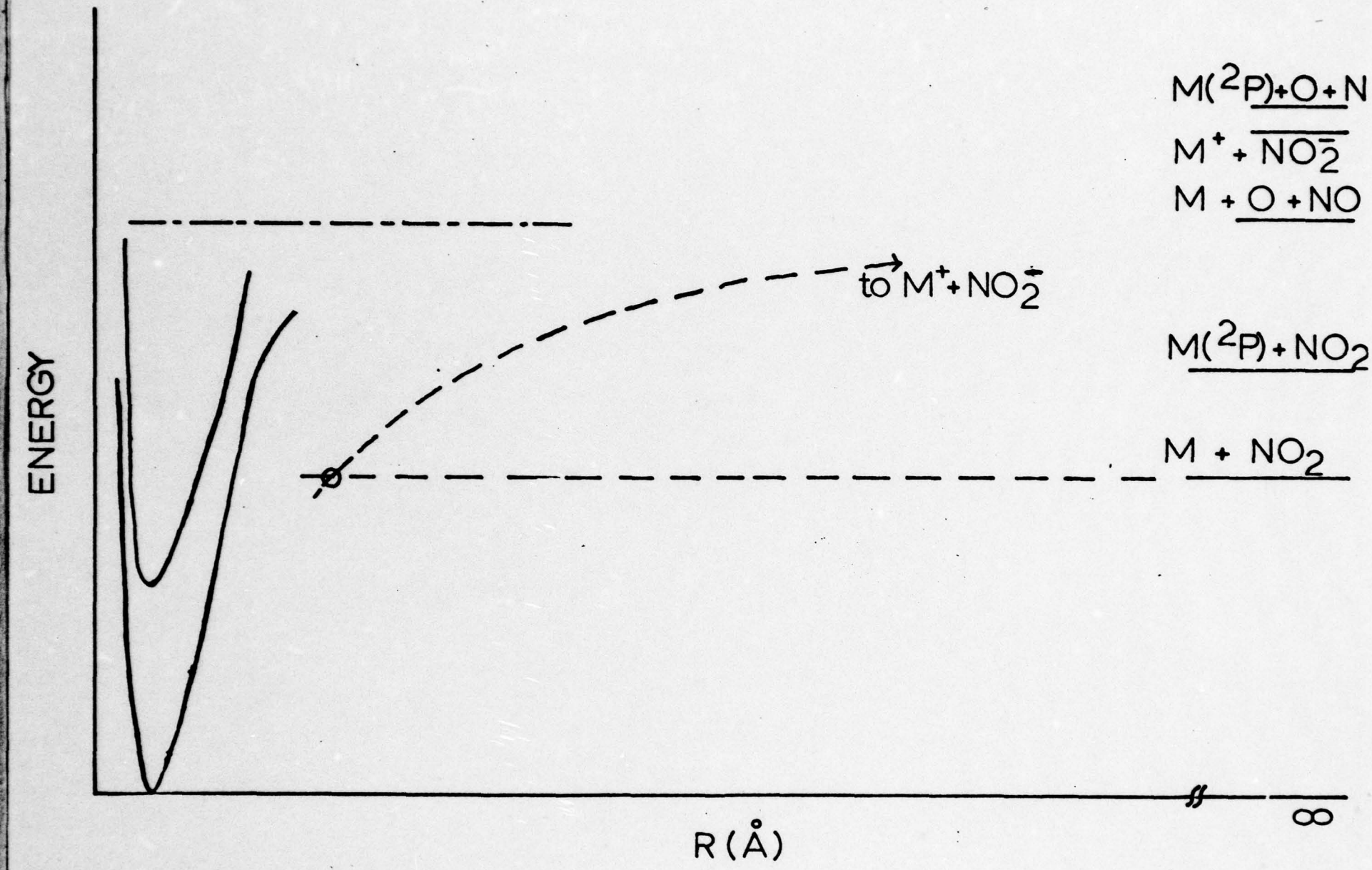

Figure 3

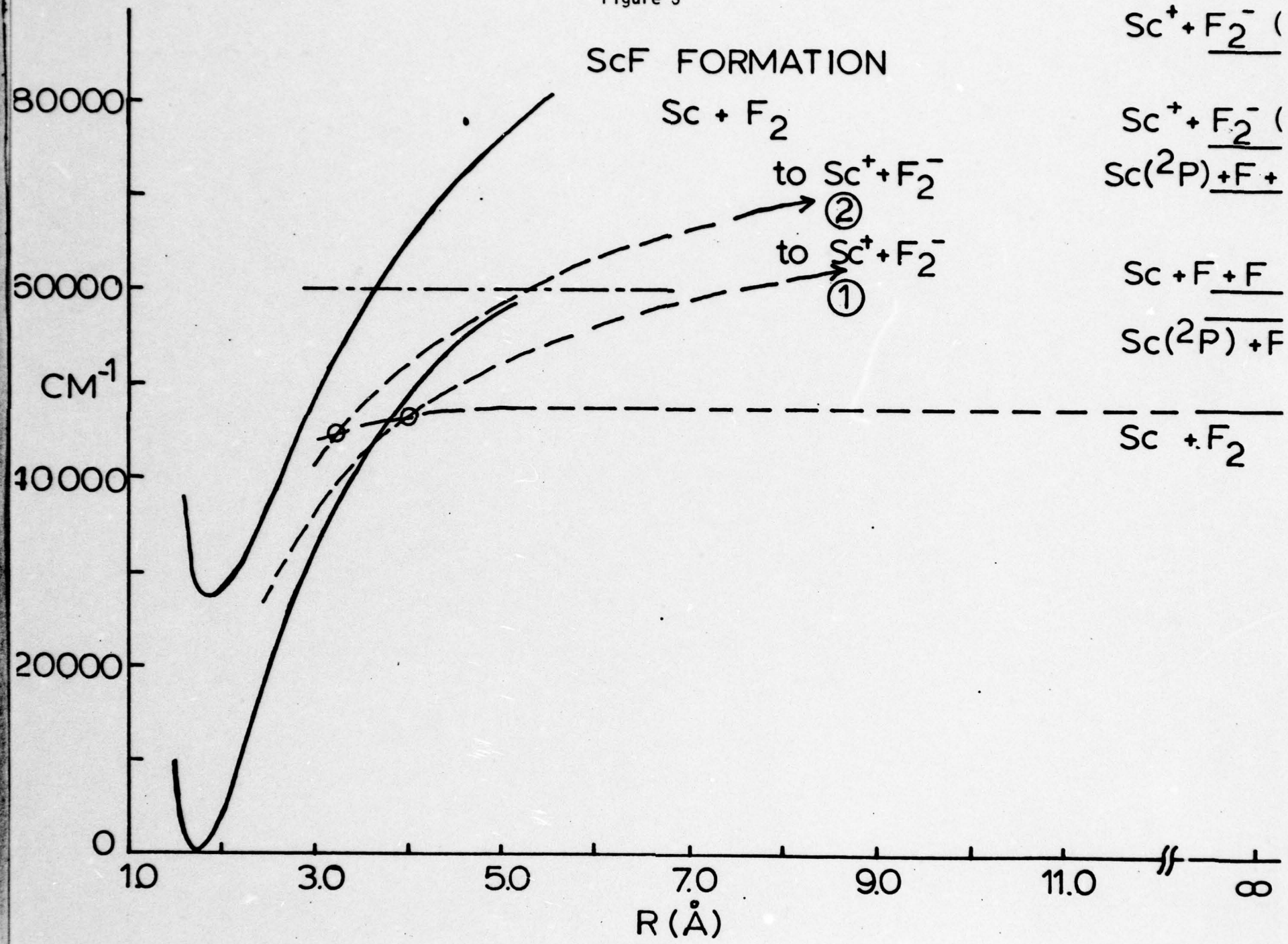
ScF FORMATION
Sc + F2
to Sc+ + F2−
②
to Sc+ + F2−
①
Sc+ + F2− (
Sc+ + F2− (
Sc(2P) + F +
Sc + F + F
Sc(2P) + F
Sc + F2
80000
60000
CM-1
40000
20000
0
1.0
3.0
5.0
7.0
9.0
11.0
∞
R (Å)

Figure 4

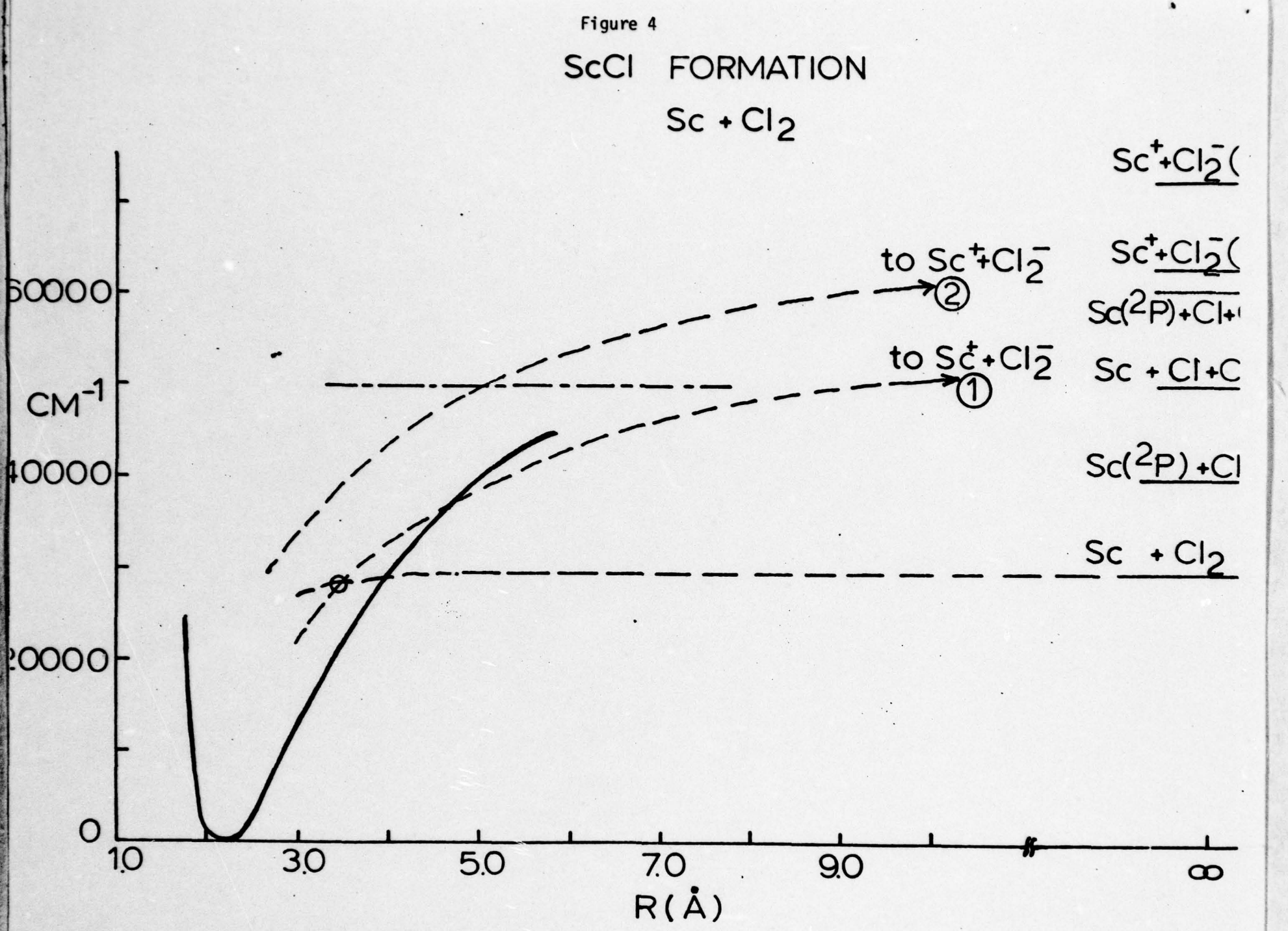
ScCl FORMATION
Sc + Cl2
Sc+ + Cl2−
to Sc+ + Cl2−
②
Sc+ + Cl2−
Sc(2P) + Cl +
to Sc+ + Cl2−
①
Sc + Cl + C
Sc(2P) + Cl
Sc + Cl2
60000
CM-1
40000
20000
0
1.0
3.0
5.0
7.0
9.0
∞
R(Å)

Figure 5

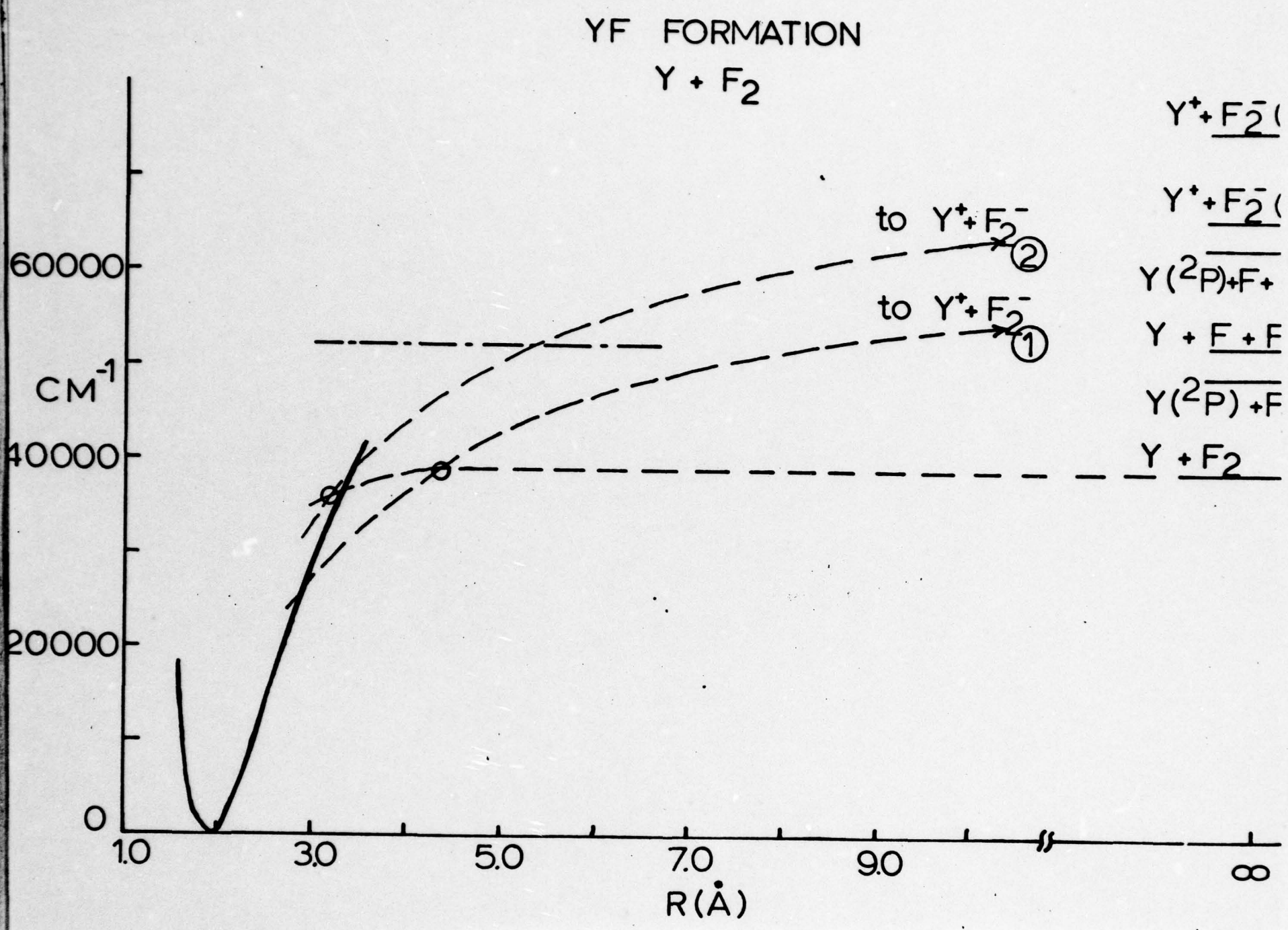
YF FORMATION
Y + F2
Y+ + F2-(
Y+ + F2-(
to Y+ + F2-
2
Y(2P)+F+
to Y+ + F2-
1
Y + F + F
Y(2P) +F
Y + F2
60000
CM-1
40000
20000
0
1.0
3.0
5.0
7.0
9.0
∞
R(Å)

Figure 6

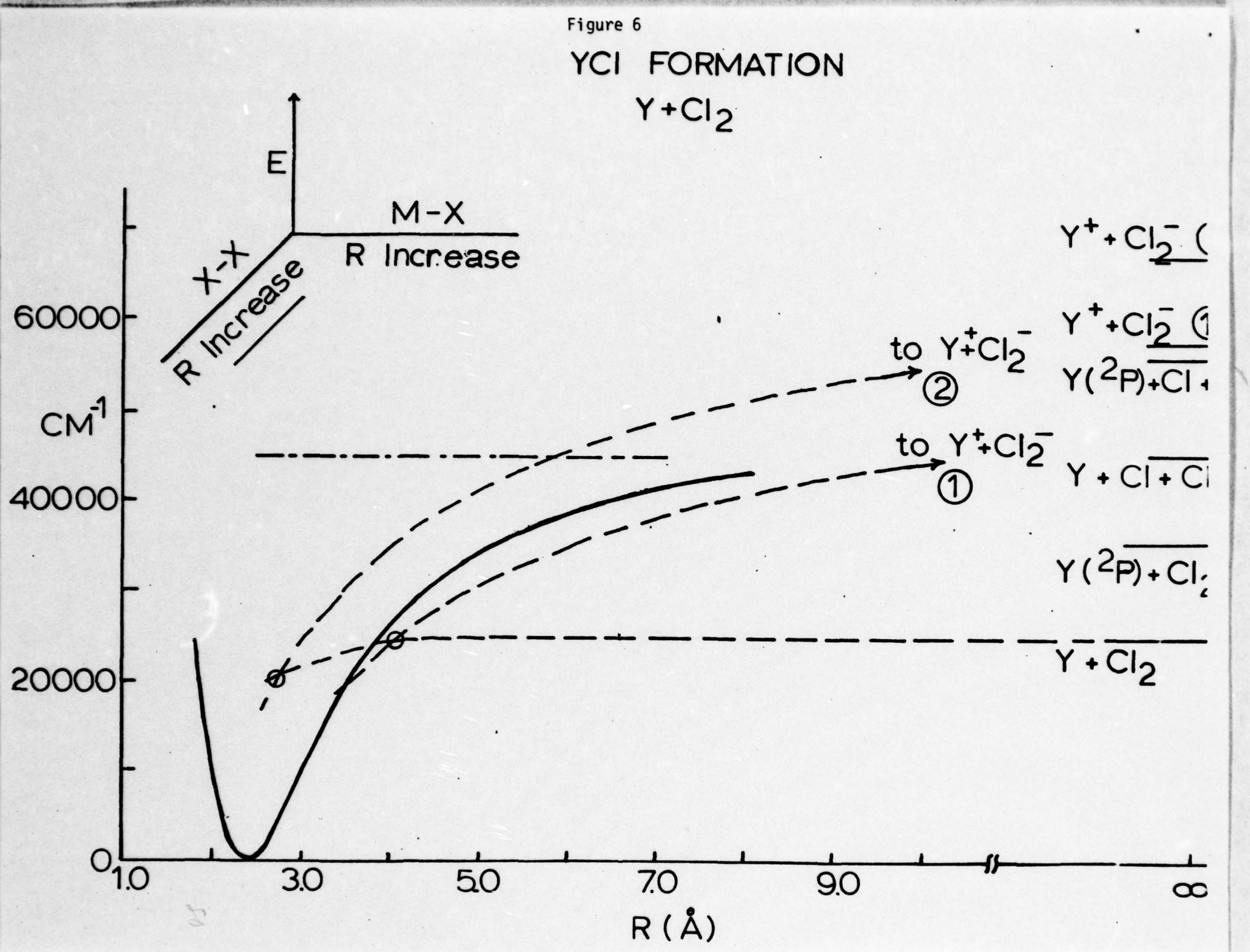
YCl FORMATION
Y + Cl2
E
M-X
R Increase
X-X
R Increase
60000
CM-1
40000
20000
0
1.0
3.0
5.0
7.0
9.0
∞
R (Å)
to Y+Cl2-
②
to Y+Cl2-
①
Y+ + Cl2- (
Y+ + Cl2- (1
Y(2P) + Cl
Y + Cl + Cl
Y(2P) + Cl2
Y + Cl2

Figure 7

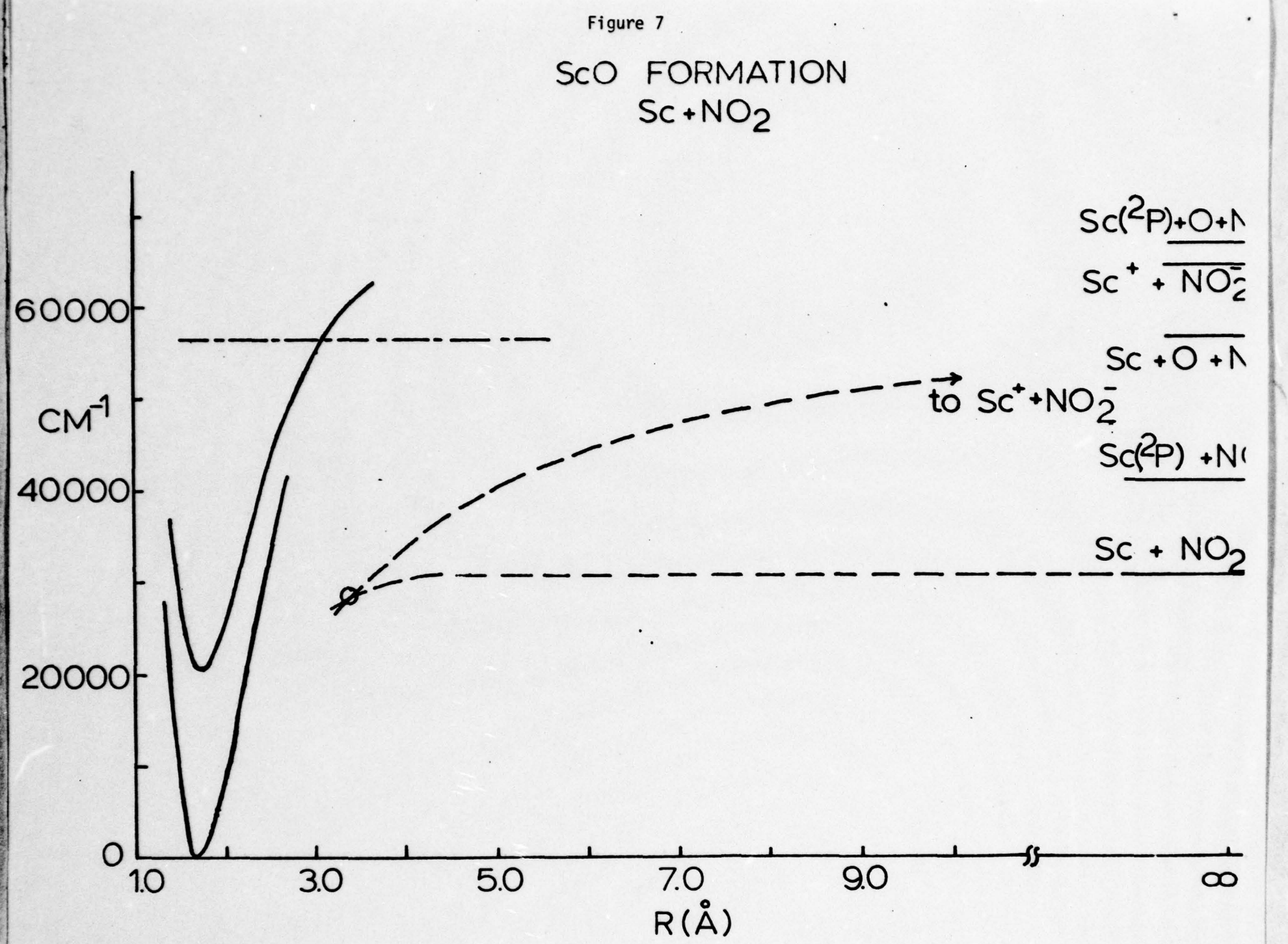
ScO FORMATION
Sc + NO2
60000
CM-1
40000
20000
0
1.0
3.0
5.0
7.0
9.0
∞
R(Å)
Sc(2P)+O+N
Sc+ + NO2-
Sc +O +N
to Sc+ +NO2-
Sc(2P) +N
Sc + NO2

Appendix B

A Comparative Study of Group IIIB - Halogen Reactions

Possible Applications to Chemical Laser Development

Metal Halide Chemistry

A COMPARATIVE STUDY OF GROUP IIIB - HALOGEN REACTIONS* POSSIBLE APPLICATIONS TO CHEMICAL LASER DEVELOPMENT

James L. Gole and Carl L. Chalek

Department of Chemistry
Georgia Institute of Technology
Atlanta Georgia 30332

and

General Electric Research and Development
Schenectady, New York 123

Chemiluminescent reactions of Group IIIB metals, scandium, yttrium, and lanthanum with F_2, Cl_2, Br_2, SF_6, ClF, IBr, I_2, and ICl have been studied under "single collision" conditions using a beam-gas arrangement. Observed chemiluminescent spectra are primarily attributed to emission from the metal monohalides. Dihalide emission is observed in the Sc-Cl_2, Sc-Br_2, and Sc-I_2 systems. The monohalide emission features for the scandium and yttrium halides are dominated by a previously unobserved "selectively formed" feature attributed to emission from a long lived $^3\Sigma^+$ state. The state is assigned on the basis of molecular orbital theory, energy conservation, and the known spectra for scandium and yttrium fluoride. We discuss mechanisms accounting for the observed monohalide emission trends and characterizing the entire grid of reactions studied. Based upon these mechanisms, the radiative lifetimes of the selectively populated states are found to be on the order of 2×10^{-3} seconds. Analysis of reaction temperature dependence reveals that "selective" excited state formation proceeds with negligible activation energy. From the short wavelength limits of the chemiluminescent spectra, lower bounds for the dissociation energies of the monohalides are determined.

As can be seen from the wide diversity of presentations in this symposium, the understanding of metal halide chemistry and kinetics and the determination of the stabilities of metal halides have a wide scope of applicability. In the present discussion, we focus on a comparative study of Group IIIB - halogen reactions. A grid of reactions has been studied under sufficiently controlled conditions so as to allow precise definition of processes producing excited states of the Group IIIB halides. A beam-gas arrangement has been used to study the emission from those product molecules formed in a "single collision" metathesis.[1] Hence, in order to observe chemiluminescence, we require a bimolecular metal oxidation whose exothermicity is sufficient to

populate some excited electronic state of the product molecule which we wish to study.

In addition to determining lower bounds[1] for the stabilities of the monohalides, we have been concerned with the applicability of these reactions to the development of a "visible chemical laser".[2] The development of such a laser system must be intimately tied to an understanding of those phenomena which give rise to visible chemiluminescence. The choice of an appropriate gain medium for a visible laser involves principally a playoff between excited state radiative lifetime, reactant mixing efficiencies, radiative quenching, and required inversion densities.[3] In order to achieve the necessary inversion density, one must deal with systems which produce chemiluminescent product molecules, having sufficiently long radiative lifetimes ($\geq 10^{-5}$ seconds)[4] while still maintaining reasonable coupling to the laser cavity.

Previously,[2,3] we have outlined an approach to the selective production of excited electronic states in chemical reaction. Briefly we have chosen to look at systems in which the molecular orbital makeup of certain excited electronic product molecule states, accessible to a chosen chemical reaction, differs substantially from the ground or low lying states of this product molecule. We ask whether this substantial change will affect the branching ratio of a chemical reaction and lead to preferential population of these excited states. In order to achieve this criteria, we focus on the oxidation of those metals whose atomic orbital makeup undergoes[5] a pronounced change upon promotion from the ground to a very "low-lying" excited electronic state. We will consider those product molecule excited states which correlate with these low-lying excited metal atom states in dissociation. It is likely that these product states will have molecular orbital makeups differing substantially from the ground or low lying states of the product molecule. In order to insure the possible population of these excited electronic product molecule states in a "single collision" bimolecular process, we also require that the resulting chemiluminescing product of metallic oxidation (preferably a diatomic molecule) have a substantial bond strength. Our bond strength requirement causes us to concentrate on metal oxide or halide formation. The situation which must arise under "single collision" bimolecular oxidation of a given metal is depicted in Figure 1. The metal halide or oxide product molecule excited states which can be populated under single collision conditions must lie at energies less than the energy difference (D_0^0(MX) - D_0^0(oxidant)). We have denoted this energy difference by a horizontal line in the figure whose separation from the dissociation asymptote of the product ground state corresponds to the bond energy of that oxidant bond broken in reaction.[5]

Our criteria are most closely fit by the metals scandium, yttrium, and lanthanum. The ground states of these metals are of ^2D symmetry (electron configurations Sc, [Ar] $4s^2 3d$; Y, [Kr] $5s^2 4d$; La,

[Xe] $6s^2 5d$) and all three atoms have "low lying" ^2P electronic states (electron configuration...s^2p). Here, from the standpoint of a single determinant description, we have a considerable change in atomic orbital makeup, from d to p atomic orbital character.[5] Our selection is based on single determinant arguments and does not take into account configuration interaction between atomic states. Nevertheless the ground ^2D and "low lying" ^2P states have considerably different atomic orbital makeups. We consider those excited molecular states which dissociate to Sc*, Y*, or La* (^2P). We expect that these excited molecular states will differ substantially in molecular orbital makeup from the ground and very low lying excited states of the metal oxides or halides. A priori, it is not clear whether these states will be formed selectively in a bimolecular chemical reaction; however this outlined approach representes a screening principle.[7]

We find that several Group IIIB - halogen reactions lead to selective production of a previously unobserved "long-lived" excited electronic state. These reactions are characterized by unusually high quantum yields and initial studies indicate low quenching cross sections for the selectively produced state. In summary, the systems which we discuss herein show a distinct possibility for fulfilling the requirements necessary for producing a visible chemical laser.

General Features of the Chemiluminescent Spectra

We have studied the chemiluminescent emission from 19 reactions of the Group IIIB metals scandium, yttrium, and lanthanum with the halogens F_2, Cl_2, Br_2, I_2, SF_6, ClF, IBr, and ICl. We summarize the reactions studied in Table I. Observed chemiluminescent spectra are primarily attributed to emission from the metal monohalide formed via the reaction

$$M + RX \rightarrow MX^* + R \qquad (1)$$

Dihalide emission is also observed in the Sc-Cl_2, Sc-Br_2, and Sc-I_2 systems. The dihalides appear to be formed in the reaction sequence

$$M + RX \rightarrow MX + R \qquad (2)$$

$$MX + RX \rightarrow MX_2 + R \qquad (3)$$

We focus on a few specific examples.

Sc + F_2, ClF, and SF_6

Figure 2 exemplifies selective excited state emission resulting from the reaction of scandium atoms and fluorine molecules. It is apparent that the emission intensity in the region from 3400 to 3800 Å

considerably exceeds that in the other accessible spectral regions. There are several known excited electronic states of ScF lying lower in energy than the ≈3500 Å system or systems. The systems which correspond to previously observed emission or absorption features involving these states are indicated in the figure. Similar emission features result from the reaction of Sc metal with ClF and SF_6 (Figure 2). The observation that this emission feature is characteristic of all three reactions leads to four conclusions:

(1) The observed selectivity is not the result of reaction exothermicity since the strengths of the bonds broken in oxidative reaction differ considerably.

(2) The observed spectra must be dominated by emission from ScF* and, of more importance, the selective feature must emanate from an excited state or excited states of ScF. This is the only possible metal halide which can be formed in common from all three reactants F_2, ClF, and SF_6. The Sc-ClF reaction is characterized by minimal ScCl formation.[3]

(3) The selective emission feature does not originate in an excited state which has been energetically inaccessible to all previous forms of excitation applied to the ScF system.[3] The currently observed emission features are found to be first order in all three oxidants. Bond energy differences among the three fluorinating agents are substantial and the SF_6 reaction is at least 40 kcals/mole less exothermic than the F_2 reaction. Combining these energetics with the consideration of the magnitude of a realistic ScF bond energy, we are led to the conclusion that the selectively excited state emits either to the ground $^1\Sigma^+$ or low lying $^3\Delta$ state of ScF.

(4) The converse of statement (3) focuses on the extremely selective nature of those reactions leading to ScF* emission. If we assume that the state which corresponds to the ScF* selective emission feature is thermodynamically barely accessible to the Sc-SF_6 reaction, the Sc-F_2 reaction should be energetically capable of exciting states whose electronic excitation is as much as 6 electron volts above the ground state. However, we find that the Sc-F_2 reaction produces relatively weak emission at wavelengths shorter than 3000 Å.[3] Formation of molecules in an excited state or states corresponding to the 3500 Å system is favored.

Y + F_2, ClF, SF_6, Cl_2, Br_2, IBr, and ICl

We also find selectivity in the emission which results from the reactions of yttrium metal with F_2 (Figure 3), ClF and Cl_2 (Figure 4). A very weak YF feature centered at 3800 Å emanates from the Y-SF_6 reaction. The emission which characterizes the yttrium-chloride reaction is also shown in Figure 4 for easy comparison with the ClF system.

Although the Y + F_2 reaction still displays some selectivity, we observe substantial emission from the $B^1\Pi$ and the $C^1\Sigma^+$ states of YF.[3] At shorter wavelengths, the chemiluminescent spectrum is characterized by emission from previously observed $^1\Pi$-$X^1\Sigma^+$ (3670-3500 Å) and $^1\Pi$-$X^1\Sigma^+$ (3400-3000 Å) YF band systems.

It is apparent that the Y + F_2 reaction is less selective than Sc + F_2. The Y + Cl_2, Y + Br_2, and Y + IBr reactions are found to be much more selective than the Y + F_2 reaction; however, some of this apparent increase in selectivity may result from differing reaction exoergicities.[3]

The Y-ClF Reaction - YCl Emission

One of the more surprising results in the present experiments is the emission spectrum resulting from the yttrium-ClF reaction. Here we find that the spectrum is dominated by emission from YCl and displays considerably weaker YF emission. This difference in emission intensity may be attributed to the nature of the band system associated with the selective feature. It can be demonstrated that the YCl [3] excited state radiative lifetime is notably less than that for YF. Hence the emission rate for the Y-Cl_2 reaction exceeds that for Y-F_2.[3,8] In contrast, the reactions of yttrium with the heavier mixed halides are dominated by emission from the excited state (YBr*, YCl*) formed via the most exothermic channel.[3]

La + F_2, ClF, SF_6, and Cl_2

In contrast to the scandium halide and yttrium halide systems, the reactions of lanthanum with F_2, ClF, Cl_2, and SF_6 show only moderate selectivity. The emission spectra characterizing the La-Cl_2 and La-ClF reactions shown in Figure 5 are exemplary.

Sc + Cl_2, Br_2, I_2

The emission spectra which characterize the Sc-Cl_2, Br_2 and I_2 reactions are exemplified in Figure 6. The Sc-Cl_2 and Sc-Br_2 reactions are characterized by a strong ≈3500 Å feature which appears to be the analogue of the feature dominating those reactions producing ScF emission. This feature is barely visible in the emission spectrum from the Sc-I_2 reaction. The three systems are characterized by a continuous emission spectrum extending from ≈3700 to 6000 Å. All efforts to resolve this emission into band systems characteristic of the metal monohalide have proved fruitless. We discuss this feature in detail elsewhere[9] where we demonstrate that it can only be attributed to emission from the metal halides. There are other subtle features which characterize the systems summarized in Table I. We refer the reader

to references 3 and 9 where a more detailed discussion is presented.

Theory of Monohalide Spectral States

Only the Group IIIB monofluorides have been widely studied. In order to discuss the theory of the Group III monohalides, we will focus on the simplest monohalide, ScF. A wide group of studies has allowed the assignment of molecular orbital configurations to several of the states with some confidence. Assignments within the simple single determinant molecular orbital description provide a reasonable and generally accepted characterization of the ground and low lying excited states of the molecule. The low lying electronic states of ScF result primarily from promotions among orbitals localized on the scandium atom. Through a consideration of the nature of these promotions, molecular orbital configurations have been assigned. In Table II we reproduce the assignments made by Brewer and Green.[10] A comparison is made with the isoelectronic TiO and ZrO molecules. We will not attempt to outline the arguments presented by these authors but will simply point out certain salient features of the Table. Refinements are discussed elsewhere.[3,11]

The ground electronic state of ScF is clearly ionic. Because the molecule is best written Sc^+F^-, we denote the ground state configuration as $(s\sigma)^2$ on scandium. Here, an electron has been removed from the singly occupied d orbital on the scandium atom and transferred to the fluorine atom. Orbital promotions in fluorine and especially F^- (isoelectronic with neon) require large amounts of energy. Hence they are not expected to enter into a description of the low lying electronic states of the ScF molecule. We consider the known excited states and the possible promotions which can give rise to these states. To first approximation, Table II is correct.[11] One expects that the lowest lying s-d configuration will be $s\sigma d\delta$ followed by $s\sigma d\pi$ and $s\sigma d\sigma$. Similarly, for the s-p configurations $s\sigma p\pi$ is expected to lie below $s\sigma p\sigma$.

Identification of the Selectively Emitting Excited State

Two important missing states in the Brewer-Green Table are the $^1\Sigma^+$, and $^3\Sigma^+$ states resulting from the molecular orbital configuration $\ldots s\sigma 4p\sigma$. These Σ states should occur at energies somewhat higher than the $^1\Pi$ and $^3\Pi$ states resulting from the $s\sigma p\pi$ configuration. The selective feature in ScF peaks at $\sim$3500 Å and extends to longer wavelengths. Although the analysis of this new emission feature is continuing, only two definite experimental observations can be made at present. Because of the short wavelength onset of emission is the same for the F_2, ClF, and SF_6 systems ($\simeq$3400 Å -- Figure 2), and the emission appears to extend to longer wavelengths, we infer that the vibrational

frequency for the upper state must be less than that for the lower state to which the emission terminates. This lower state may be either the ground, $^1\Sigma^+$, or very low lying $^3\Delta$ electronic state of ScF. Because of a seemingly high density of states, the narrow region over which the spectrum (selective feature) extends, and the difficulties faced in resolving the spectrum, it would appear that the emission is characterized by band sequences as opposed to progressions.

Through comparison with the known singlet and triplet absorption and emission features previously observed for ScF and YF, we conclude that this study represents the first observation of emission from the excited electronic state leading to the observed selective feature.

We postulate that the observed selective feature is due to emission from either the $^1\Sigma^+$ or $^3\Sigma^+$ states resulting from the...sσ4pσ configuration. The following facts support this postulation.

(1) The $^1\Sigma^+$ and $^3\Sigma^+$ states resulting from the sσpσ configuration should lie at somewhat higher energy than the $^1\Pi$ and $^3\Pi$ states resulting from the sσpπ configuration (Table II) and the $^3\Sigma^+$ state should lie lower than the $^1\Sigma^+$ state. The $^1\Pi$ state corresponding to sσpπ lies at 26.8×10^3 cm^{-1} = 3731 Å. This is approximately the long wavelength limit of the observed selective feature in ScF, and because the excited state vibrational frequency is less than that of the ground $^1\Sigma^+$ state, we expect to observe emission from this system at wavelengths longer than 3731 Å. In contrast, the selective feature peaks at 3500 Å = 28570 cm^{-1} and extends to 3700 Å. Therefore the selective feature is approximately 2000 cm^{-1} higher in energy than the observed $^1\Pi$ emission feature. This leads us to believe that the selective feature is due to emission from the $^3\Sigma^+$ electronic state resulting from the sσpσ configuration.

(2) The known singlet states of YF are listed in Table III. The observed selective feature in YF peaks at 3800 Å (Figure 3). This corresponds to a frequency of ≈26300 cm^{-1}. We compare the energy of this selective feature to the $^1\Sigma$ state at 27989.9 cm^{-1}. The excited states of the scandium and yttrium atom are quite similar and therefore the energies of the excited states of ScF and YF are expected to be quite similar. There is no possibility that the $^1\Sigma$ emission feature emanates from an excited state other than that resulting from the sσpσ configuration in YF. For this reason, it is reasonable to assign the selective feature in YF as resulting from a $^3\Sigma^+$ excited electronic state. Its separation from the $^1\Sigma^+$ feature is a very reasonable 1700 cm^{-1}.

We conclude that the observed selective emission features correspond to emission from a $^3\Sigma^+$ state resulting from the molecular orbital configuration...sσ4pσ. This is true for both ScF and YF.

Dependence of Chemiluminescent Intensity on Oxidant Pressure

The focus of the oxidant pressure dependence studies is the selective emission feature observed in many of the Group III - halogen reactions. Figure 7 corresponds to the oxidant pressure dependence behavior observed for the chemiluminescence features characterizing the Sc-F_2, -ClF, -SF_6, and -Cl_2 reactions. The chemiluminescence intensity is plotted in arbitrary units normalized to the figure. Considering the attenuation effects which an increase in gas pressure has on the metal beam, a first or second order process is said to display a pressure dependent intensity of the form $pe^{-\alpha p}$ or $p^2e^{-\alpha p}$ where $e^{-\alpha p}$ is the beam attenuation parameter and α is proportional to the total phenomenological cross section for reactive, inelastic, and elastic scattering of the beam. The reactions producing ScF* are characterized by a linear dependence and hence a $pe^{-\alpha p}$ behavior (note the attenuation of the ScF* emission from the Sc-ClF reaction). The three reactions which produce the monofluoride are monitored at ~3500 Å. In contrast to the reactions producing ScF* emission, the pressure dependence plots for the selective ScCl* emission feature are not characterized by a totally linear behavior. Rather we observe a slight linear onset followed by a nonlinear increase in chemiluminescent intensity. The pressure dependence is of the form $p^\beta e^{-\alpha p}$ where $\beta > 1_\delta$ Similarly, the Sc-Br_2 system is characterized by a selective (~3500 Å) ScBr* emission feature displaying a faster than first order dependence. A more complete discussion of this representative behavior is provided elsewhere;[3,12,13] however, two important points can be made.

(1) The characteristic of a "faster than first order" dependence is the result of collision enhanced emission from within the excited molecular electronic state.[12] In the example presented (ScCl) a collision with the emitting excited state causes deactivation to a set of ro-vibronic levels which as a whole emit more rapidly than the nascent products formed in reaction. Deactivation causes the predominantly $^3\Sigma^+(\Omega = 1)$ state to gain $^1\Pi(\Omega = 1)$ character and thus increases the emission rate.

(2) If a molecule is formed in state A and undergoes collision enhanced emission from this state, the emission intensity is given by

$$I = S_A \left(\frac{1}{\tau_c} \int_o^{\tau_f} e^{-t/\tau_c}\right) dt$$

$$= [X_2]\,[Q]$$

where S_A = rate of formation of molecules in state A

τ_c^{-1} = collision induced emission rate from state A

τ_f = transit time of molecules through observation zone

90

X_2 = oxidant

Q = quencher

In this particular case, one observes a quadratic dependence when $\tau_c = \tau_s$, the lifetime of the A-X transition, or when the collision frequency is comparable to the radiative lifetime. Hence one can obtain an estimate of the radiative lifetime. In analyzing the break from a linear behavior for the ScCl* selective emission feature, we find the quadratic dependence to be evident at pressures on the order of 8×10^{-5} torr or lower. This allows us to estimate the excited state radiative lifetime as $\simeq 1.3 \times 10^{-3}$ seconds, assuming typical cross sections for inelastic collision. This lifetime is typical of these systems.[14]

Quantum Yield Determinations

Using a standard lamp and calibration configuration described elsewhere,[15] we have determined the quantum yields for several Group IIIB metal oxidations. In order to determine reliable quantum yields, it is necessary that we correct for all factors inherent in our optical configuration and determine the entire spectrum correcting for photo-tube spectrometer response. Using our calculated calibration curve, summing over the entire spectrum and correcting for frequency, we find the quantum yields given in Table IV.

The quantum yield is defined as the ratio of excited state emitters/total product molecules formed. While the quantum yields for Group IIIB oxide and Group IIA halide formation are quite small in general, being on the order of 10^{-1} to 10^{-3}%, Group IIIB halide formation proceeds with a quantum yield at least two orders of magnitude larger.

Because of the nature of our determination, the quantum yields obtained represent a definite lower bound to this quantity. The quantum yields obtained for the halides are unusually high for a single collision process. This high quantum yield is typical for the Group IIIB - halogen systems.[15] In contrast, the reactions producing the metal oxides and the Group IIA halides are characterized not only by relatively low quantum yields but also by relatively non-selective emission.

Activation Energies

In order to study temperature dependences, we rely on a recent formulation which relates the temperature dependence of the chemiluminescence intensity to the parameters of the beam-gas experiment.[16] The appropriate relationships are

$$-R\,\frac{d(\ln I)}{d(1/T_B)} = \Delta H_{vap} + [d(1/T_{eff})/d(1/T_B)][E_{exp}] - RT_B \qquad (4)$$

$$E_{exp} = -d[R\ln(IT_B) + \Delta H_{vap}\,(T_B^{mean})/T_B]/d(1/T_{eff}) \qquad (5)$$

where

I = chemiluminescence intensity

T_B = metal beam temperature

E_{exp} = activation energy for formation in a given vibrational level of the excited electronic state

m_B = the mass of a Group III atom

m_G = the mass of a halogen molecule

$T_{eff} = [m_B(T_G) + m_G(T_B)]/[m_G + m_B]$

T_G = the oxidant gas temperature, 300 K

T_B^{mean} = the mean temperature over the experimental temperature range

ΔH_{vap} is evaluated at the mean temperature of the experimental run.

We have summarized measured activation energies for several reactions forming metal oxide and metal halide excited states in Tables V and VI. With the exception of YO ($A'^2\Delta$) production via the $Y-O_2$ reaction, all metal oxide forming reactions proceed with non-negligible activation energies.[16] Many of the reactions of the Group IIIB metals with the halogens lead to selective formation of the previously unobserved long lived[3,12] $^3\Sigma^+$ excited state of the metal monohalide. In contrast to those processes leading to excited state metal oxide formation, we find negligible activation energies for formation of this $^3\Sigma^+$ state.[3,17] As is apparent from Table VI, this is not a trend characteristic of metal monohalide formation in general, but rather reflects the nature of processes corresponding to formation of specific excited states. The reaction resulting in formation of the YF C $^1\Sigma^+$ state proceeds with a substantial activation energy.[3] In Table VI, we also present the results of our temperature dependence studies on the $Ca + F_2 \rightarrow CaF^* + F$ and $Sr + F_2 \rightarrow SrF^* + F$ reactions. Excited state formation in these reactions also proceeds with a substantial activation energy.

The negligible activation energy for those processes producing the selective monohalide emission features indicates that we are observing a direct process for formation in those excited states from which emission is observed. A complete analysis of the temperature dependence for the summarized reactions using equation (4)[3,7,16] can be applied to demonstrate that all metatheses proceed with ground state atoms.

Dissociation Energies for Metal Monohalides

The initial bimolecular metathesis resulting in formation of the Group IIIB metal monohalide (eg. (1)) results in an emission spectrum unaltered by subsequent collisional deactivation.[18] We can deduce a lower bound to the monohalide bond dissociation energy from the short wavelength limit of this chemiluminescent spectrum. Using the selective emission feature for which our temperature dependent studies yield a negligible activation energy,[19] and considering the nature of the energy conservation entailed in the bimolecular reaction of ground state metal atoms (temp. dep.), we arrive at an expression for the dissociation energy of the metal monohalide.

Focus on the gas phase bimolecular reaction of ground state metal atoms, M = Sc(^{2}D), Y(^{2}D), and La(^{2}D) with halogen molecules viz.

$$M(^2D) + X_2(^1\Sigma_g^+) + E_T^i \rightarrow MX(\ ,v') + X(^2P) + E_T^f \qquad (6)$$

Here scandium, yttrium, and lanthanum atoms, M, thermally distributed throughout the fine structure components of the ^{2}D state, and halogen molecules in their ground state collide with relative initial translational energy E_T^i (measured in the center of mass frame) to form excited MX molecules and ground state X(^{2}P) atoms with relative final translational energy E_T^f.

Conservation of energy requires that all forms of energy on the right-hand side of equation (6) exactly balance all forms of energy on the left-hand side. Choosing M(^{2}D, J = 3/2) + X(^{2}P, J = 3/2) + X_2 ($X^1\Sigma_g^+$, v' = 0) to be the reference energy, we may write

$$-D_0^0(X_2) + E_{int}(X_2) + E_{int}(M) + E_T^i = -D_0^0(MX) + E_{int}(MX) + E_{int}(X) + E_T^f \qquad (7)$$

where $E_{int}(M)$, $E_{int}(X_2)$, $E_{int}(X)$, and $E_{int}(MX)$ are the average internal energies (electronic, vibrational, rotational) of M atoms, X_2 molecules, X atoms, and MX molecules, respectively, measured with respect to the lowest energy level of each species. The energy sum $E_{int}(X) + E_T^f$ is unknown and cannot be obtained from the chemiluminescent spectrum. Therefore, we obtain the inequality

$$D_0^0(MX) \geq D_0^0(X_2) + E_{int}(MX) - [E_{int}(X_2) + E_T^i + E_{int}(M)] \qquad (8)$$

Because we have not resolved the selective emission feature for the Group III monohalides, we obtain a lower bound for $E_{int}(MX)$ by converting the short wavelength limit of the observed spectrum to an energy increment. If the short wavelength feature which we observe in the spectrum corresponds to emission from the highest excited state quantum level populated in the reaction and the emission terminates in

the lowest ($v'' = 0$, $J'' = 0$) vibrational-rotational level of the ground electronic state, $E_{int}(MX)$ provides a good estimate of the heat of reaction.[20] By virtue of our method of determination, the calculated $E_{int}(MX)$ in the present study represents a definite lower bound.[21] The evaluation of $E_{int}(X_2)$, $E_{int}(M)$, and E_T^i are discussed in the literature.[22-24]

In Table VII we present calculated values for $E_{int}(M)$, $E_{int}(MX)$, E_T^i, and $E_{int}(X_2)$. From these quantities we calculate minimum dissociation energies for the fluorides, chlorides, and bromides of the Group IIIB metals.

The previous data on the Group IIIB metal halides is sparse; only the ScF and YF bond energies have been determined.[27] From our studies with SF_6, we find notably higher dissociation energies than those obtained by previous workers.[25] The value for ScF must be viewed as tentative and must await further temperature dependent studies. The determined values for the F_2 and ClF oxidations yielding the fluorides will probably increase substantially when resolved spectra are obtained.

There appear to be two clear trends: 1) dissociation energies decrease in the order fluorides > chlorides > bromides, and 2) this decrease is least pronounced for the lanthanum compounds and substantial for both the scandium and yttrium halides.

Proposed Model for Selective Excitation

We believe that the selective emission features characterizing the Group IIIB - halogen reactions and the relatively non-selective emission which characterizes formation of many Group IIIB oxides[2,24] can be qualitatively explained within the framework of the familiar electron jump model.[26]

In the traditional electron jump model, reaction is initiated as a valence electron of the metal atom, M, is transferred to the oxidant molecule with which reaction takes place. Subsequent interaction of M^+ with the oxidant leads to product formation. Refinements of the electron jump model have recently been discussed by Kinsey;[27] however, we adopt the simplified picture of the electron jump mechanism. Here the covalent curve, M + (oxidant) crosses the ionic curve M^+ + $(oxidant)^-$ at a distance r_c given by

$$r_c(A) = \frac{14.38}{I.P.(M) - E.A.(oxidant)} \qquad (9)$$

where I.P.(M) is the ionization potential of the metal atom, in this case scandium, yttrium, or lanthanum, and E.A. (oxidant) is the vertical electron affinity of the oxidant molecule. These energies are expressed in electron volts.

For the overwhelming number of cases, the electron jump which takes place leads to formation of the ground electronic state of that product molecule formed in reaction. One usually finds that the ionic curve corresponding to the ground electronic state of the product molecule crosses the M + (oxidant) curve at a larger internuclear distance than do those curves corresponding to any ionic excited electronic states. In most cases, this means that the electron jump mechanism will lead predominantly to production of ground state molecules.[26,27]

The large cross sections and negligible activation energies[1] for formation of electronically excited Group IIIB halides strongly suggest that the M + RX reactions selectively populate (an) excited electronic state(s) by direct formation of MX*. In contrast, the M + RO → MO* + R reactions apparently do not proceed via this direct mechanism, but rather excited state formation occurs as a result of rearrangement from a ground state M^+ $(oxidant)^-$ complex or high vibrational levels of the product molecule ground state, both being indirect routes.[16] The difference in the magnitude of the cross section for excited state formation which characterizes the two classes of reactions may be understood in a qualitative sense upon examination of the metal-oxidant interaction potentials and approximate molecular electronic potential curves characterizing the metal oxide or metal halide molecule which is formed.

Employing available spectral data for the Group III halides and oxides and generating potential curves using the technique of Pade approximants,[28] we distinguish two distinct situations. They are represented schematically in Figures 8 and 9. These two "limiting cases" correspond to two superimposed planes of the reaction hypersurface. The selective M + X_2 reactions appear to be characterized by an electron jump crossing radius, r_c, at considerably smaller internuclear distance than the outer turning point of the ground state potential. The electron jump occurs at an internuclear distance such that direct transfer into the ground electronic state of the product monohalide is either negligible or is such that a strong competition for formation of ionic excited electronic states also exists. In other words, direct excited state formation appears to be facilitated. In contrast, Figure II corresponds to a relatively non-selective reaction involving the production of a metal oxide. Here the electron jump takes place at sufficiently large internuclear distance versus the location of the metal oxide potential curves that formation of the ionic ground state is favored. In summary, selective reactions appear to be characterized by an electron jump to (the) excited state(s) while non-selective reactions involve the traditional jump to the ground ionic state. One might envision the selective process as a "scoop" mechanism whereby the ionic excited electronic states are effectively the first ionic states to which the M^+ $(oxidant)^-$ complex is exposed during the course of reaction. We believe that the selectivity and high quantum yields for the Group

IIĪ - halogen reactions are due primarily to the nature of the electron jump process and secondly to the sp molecular orbital makeup of those states formed selectively. We must note that the magnitude of the selectivity which is apparent from the spectral scans (Figures 2-4) is probably underestimated because of the long radiative lifetime characterizing the selectively formed $^3\Sigma^+$ excited state.[3] A confirmation of this point must await the direct measurement of a radiative lifetime for both selective and non-selective features and hence a comparison of relative decay rates across the observation region. Further discussion of this proposed model is provided elsewhere.[3]

References

*This work supported in part by the Air Force Office of Scientific Research.

1. J.L. Gole, Ann. Rev. Phys. Chem. 1976 27:525-51.

2. L.J. Gole in Proceedings of the Second Summer Colliquium on Electronic Transition Lasers, Edited by S.N. Suchard, L.E. Wilson, and J.I. Steinfeld, pp. 136-165.

3. James L. Gole and Carl L. Chalek, Beam-Gas Chemiluminescent Reactions of Group IIIB Metals and Halogen Molecules - Evidence for Selective Excited State Emission (in press).

4. A radiative lifetime of 10^{-5} seconds is comparable to the time for intimate reactant mixing at 6 torr, the typical operating pressure for a useful chemical laser system.

5. Here, we refer to the single determinant Hartree-Fock description of the metal atom.

6. Because of the distribution in translational energy characterizing the metal beam, this horizontal line is in reality an energy band.

7. The presence of the ionic ground state (M^+ $(...s^2)$ X^- $(...p^6)$) does not affect our discussion of orbital change. If anything, it complements the desired character we seek for gound and excited states; that is a substantial change in molecular orbital character. There are many low lying molecular states which can also correlate with the ground state neutral products (M^2D) + $X(^2P)$, and these states may effectively saturate the available d orbital character from the metal atom. Therefore we preserve our change from d to p orbital character because those states correlating with $M(^2P)$ + $X(^2P)$ will be characterized by substantial p orbital character while possessing little d orbital character from the metal atom.

8. It appears that the YCl, YBr, and YI molecules are characterized by a much stronger coupling of spin and orbital angular momentum than is YF. Therefore the $\Delta\Sigma = 0$ selection rule characterizing Hund's cases (a) or (b) breaks down and the observed transition becomes more allowed.

9. James L. Gole, "A Comparative Study of Group IIIB - Halogen Reactions. II. Observation of $ScCl_2$*, $ScBr_2$*, and ScI_2* Chemiluminescence.

10. L. Brewer and D.W. Green, High Temperature Sciences 1, 26 (1969).

11. P.R. Scott and W.G. Richards, Chem. Phys. Lett. 28, 101 (1974).

12. J.L. Gole, D.R. Preuss and C.L. Chalek, J. Chem. Phys. 66, 548 (1977).

AD-A065 156 GEORGIA INST OF TECH ATLANTA DEPT OF CHEMISTRY F/G 20/5
SELECTIVE CHEMICAL PUMPING OF ELECTRONIC STATES AND FORMATION A--ETC(U)
1978 J L GOLE AFOSR-78-3515
UNCLASSIFIED AFOSR-TR-79-0102 NL

2 OF 2
AD
A065156

END
DATE
FILMED
4-79
DDC

13. We observe a pressure dependence of the form $p^{\beta}e^{-\alpha p}$ for the reactions forming YCl, YBr, YI, ScCl, ScBr, ScI, and LaCl.

14. N.F. Ramsey, Molecular Beams (Oxford U.P., London, 1969).

15. C.L. Chalek and J.L. Gole, "A Comparative Study of Excited State Cross Sections for Group IIIB Halide and Oxide Production - Lower Bounds for Excited State Quantum Yields" - following paper.

16. D.R. Preuss and J.L. Gole, J. Chem. Phys. 66, 2994 (1977), J. Chem. Phys. 66, 3000 (1977).

17. The error bounds quoted in Table VI are substantial and in many cases exceed the quoted activation energies by several kcals/mole. These error bounds are not meant to imply the possibility of a negative activation energy;[29] rather they may indicate a complicated set of curve crossings in the region where the nature of the excited state curves is such that direct passage into excited states occurs. Further discussion of this point will be presented in the third paper in this series.

18. The rotational relaxation which accompanies typical inelastic collisions with metastables corresponds to a ΔJ change on the order of 10. This change will have a negligible effect on the observed spectrum. For the systems considered reaction products undergo a maximum of one collision before emitting monitored radiation. See also reference 12.

19. That is the activation energy correction to the dissociation energy will be negligible. For a discussion of the correction, see D.R. Preuss and J.L. Gole, J. Chem. Phys. 66, 880 (1977).

20. Lawrence H. Dubois and James L. Gole, J. Chem. Phys. 66, 779 (1977).

21. See for example C.R. Dickson and R.N. Zare, Chem. Phys. 7, 361-370 (1975) and references therein.

22. J.L. Gole and R.N. Zare, J. Chem. Phys. 57, 5331 (1972).

23. P.J. Dagdigian, H.W. Cruse, and R.N. Zare, J. Chem. Phys. 62, 1824 (1975).

24. C.L. Chalek and J.L. Gole, Chem. Phys. 19, 59-91 (1977).

25. K.F. Zmbov and J.L. Margrave, J. Chem. Phys. 47, 3122 (1967).

26. D.R. Herschbach, Adv. Chem. Phys. 10, 319 (1966).

27. J.L. Kinsey, "Molecular Beam Reactions" in "Biennial Reviews of Science, Technology, and Medicine, Reaction Kinetics Volume 9", Chapter 6.

28. K.D. Jordan, J.L. Kinsey and R. Silbey, J. Chem. Phys. 61, 911 (1974).

29. James L. Gole and Carl L. Chalek, J. Chem. Phys. 65, 4384 (1976).

Figure Captions

Figure 1. Qualitative description of energy conservation in a single collision bimolecular chemiluminescent reaction forming a Group IIIB metal oxide or halide.

Figure 2. Chemiluminescent emission from the reactions Sc + F_2 → ScF* + F, Sc + ClF → ScF* + Cl, and Sc + SF_6 → ScF* + SF_5. Regions of previously observed emission or absorption features are identified in the Figure. A = Absorption, HC = Hollow Cathode Discharge. The observed emission including the region from 3800 Å to 6200 Å is due entirely to metal monofluordie emitters. Note the relative intensities given in Figure 10.

Figure 3. Chemiluminescent emission from the reaction Y + F_2 → YF* + F. Regions of previously observed emission or absorption features are identified in the Figure. A = Absorption.

Figure 4. Chemiluminescent emission from the reaction Y + ClF → YCl* + F or YF* + Cl and Y + Cl_2 → YCl* + Cl. The baseline of the Y-ClF spectrum is slightly shifted for comparison. The Y-ClF emission spectrum is dominated by YCl* emission from the selectively populated $^3\Sigma^+$ state of YCl.

Figure 5. Chemiluminescent emission from the reactions La + ClF → LaF* + Cl + LaCl* + F and La + Cl_2 → LaCl* + Cl. Regions of previously observed emission or absorption features are identified in the Figure.

Figure 6. Chemiluminescent emission from the reaction Sc + Cl_2 → ScCl* + Cl and Sc + $2Cl_2$ → $ScCl_2$* + Cl_2. The indicated transitions throughout the spectrum correspond to known regions of ScCl emission; however, it is doubtful that spectral features corresponding to previously known states of ScCl are observed. The 3500 Å feature corresponds to emission from the $^3\Sigma^+$ state of ScCl and the continuum from ~3500 Å to 6000 Å corresponds to $ScCl_2$ emission. See text for discussion.

Figure 7. Chemiluminescent intensity versus oxidant pressure for the reactions of Sc with F_2, ClF, Cl_2, and SF_6. Intensities are normalized to the Figure .

Figure 8. Qualitative description of potential energy curves and interactions for selective excited state formation.

Figure 9. Qualitative description of potential energy curves and interactions for non-selective excited state formation.

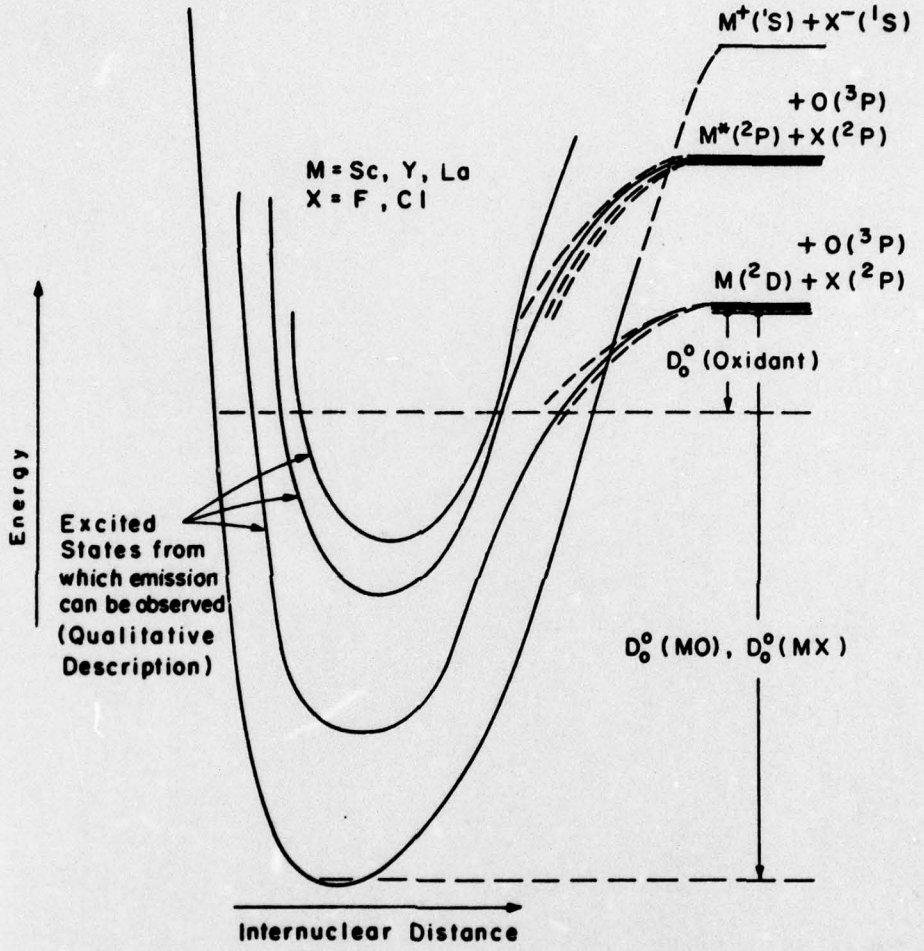
$M^+(^1S) + X^-(^1S)$
$+ O(^3P)$
$M^*(^2P) + X(^2P)$
M = Sc, Y, La
X = F, Cl
$+ O(^3P)$
$M(^2D) + X(^2P)$
D_0^o (Oxidant)
Energy
Excited States from which emission can be observed (Qualitative Description)
D_0^o (MO), D_0^o (MX)
Internuclear Distance

Figure 1

10 A

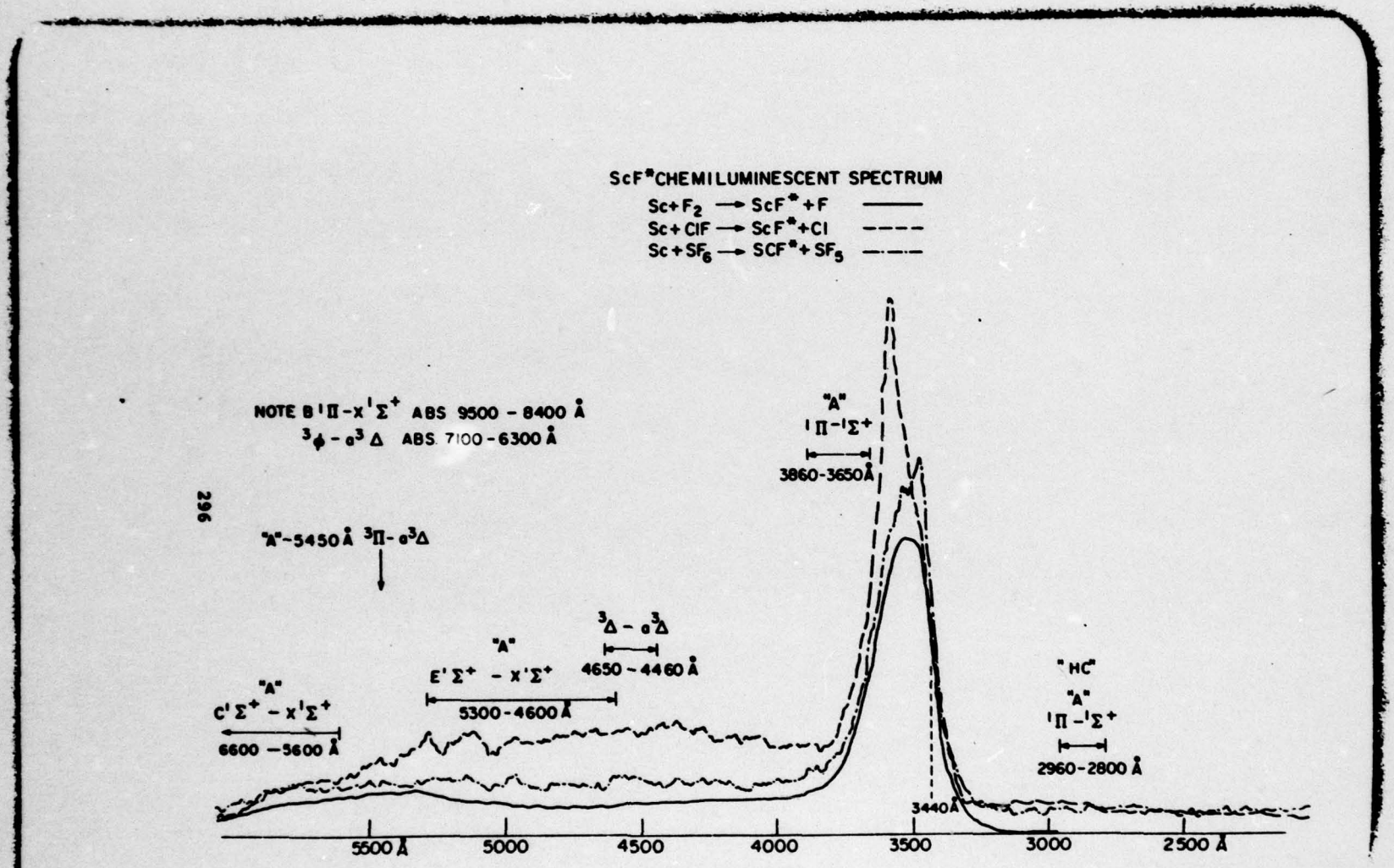
ScF* CHEMILUMINESCENT SPECTRUM
Sc + F2 → ScF* + F
Sc + ClF → ScF* + Cl
Sc + SF6 → SCF* + SF5
NOTE B 1Π - X 1Σ+ ABS 9500 - 8400 Å
3φ - a3Δ ABS 7100 - 6300 Å
"A" 1Π - 1Σ+
3860 - 3650 Å
"A" - 5450 Å 3Π - a3Δ
3Δ - a3Δ
4650 - 4460 Å
"A"
E' Σ+ - X' Σ+
5300 - 4600 Å
"A"
C' Σ+ - X' Σ+
6600 - 5600 Å
"HC"
"A"
1Π - 1Σ+
2960 - 2800 Å
3440 Å
5500 Å
5000
4500
4000
3500
3000
2500 Å

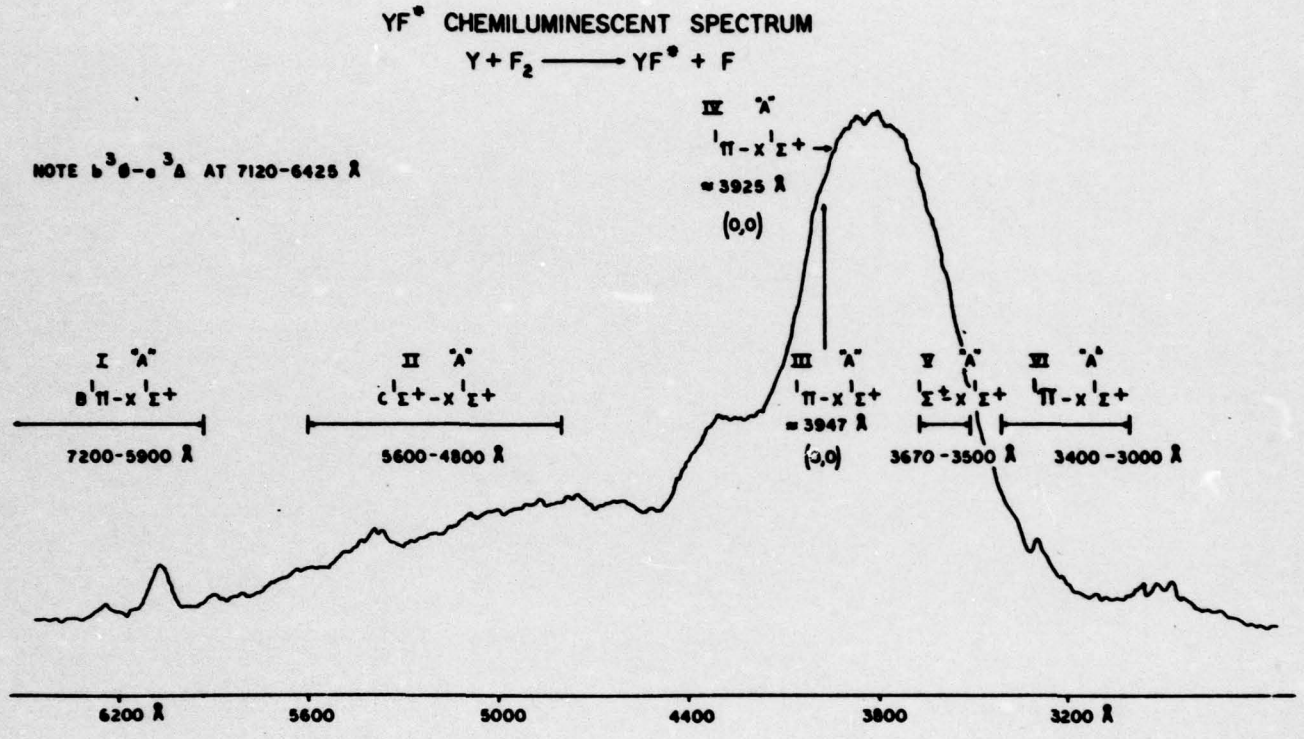
YF* CHEMILUMINESCENT SPECTRUM
Y + F2 ⟶ YF* + F
NOTE b3Θ−a3Δ AT 7120-6425 Å
IV "A"
1Π − X1Σ+
≈ 3925 Å
(0,0)
I "A"
B1Π − X1Σ+
7200-5900 Å
II "A"
c1Σ+ − X1Σ+
5600-4800 Å
III "A"
1Π − X1Σ+
≈ 3947 Å
(3,0)
V "A"
1Σ± X1Σ+
3670 - 3500 Å
VI "A"
1Π − X1Σ+
3400 - 3000 Å
6200 Å
5600
5000
4400
3800
3200 Å

Figure 3

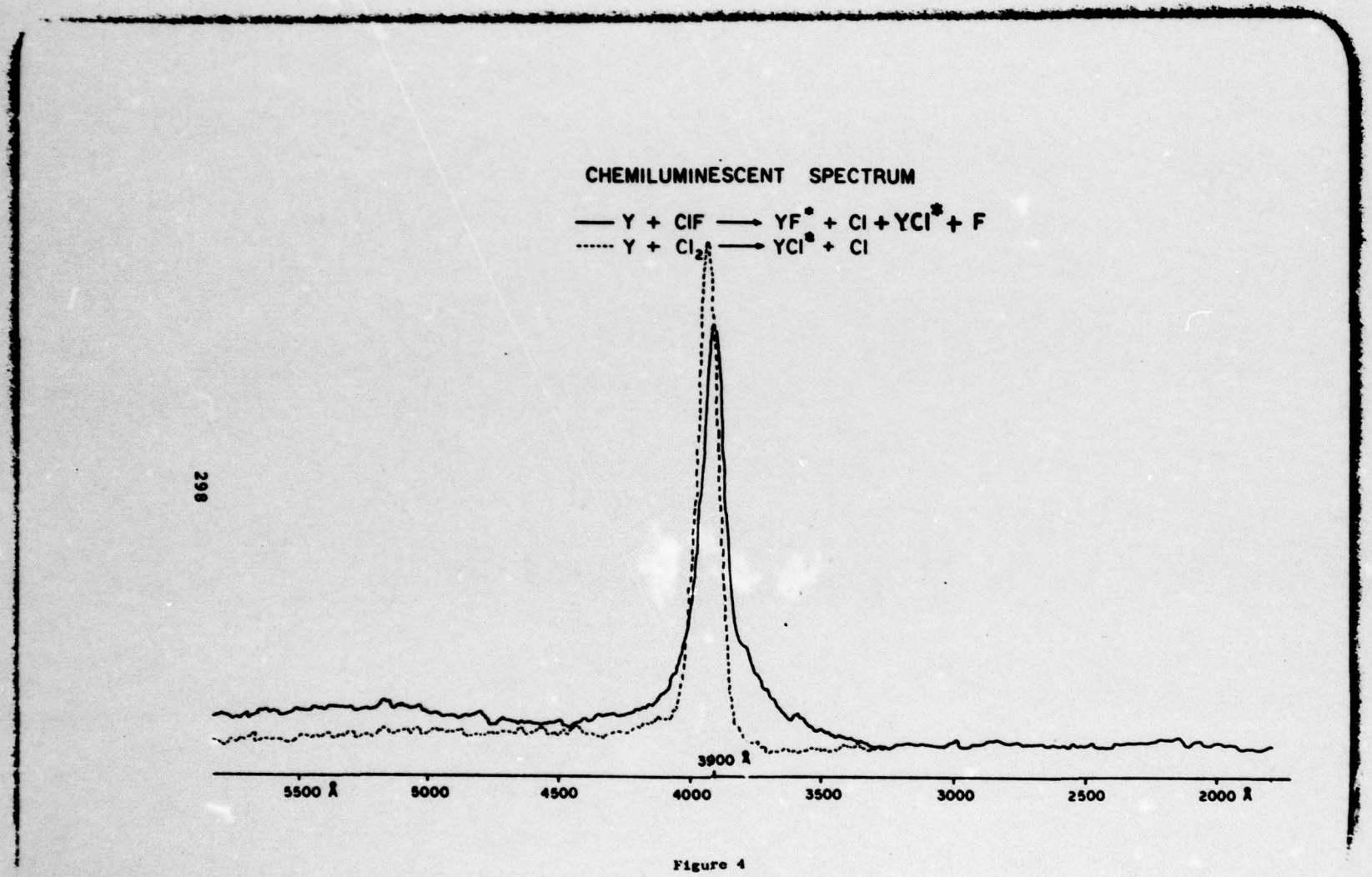
CHEMILUMINESCENT SPECTRUM
Y + ClF → YF* + Cl + YCl* + F
Y + Cl2 → YCl* + Cl
3900 Å
5500 Å
5000
4500
4000
3500
3000
2500
2000 Å

Figure 4

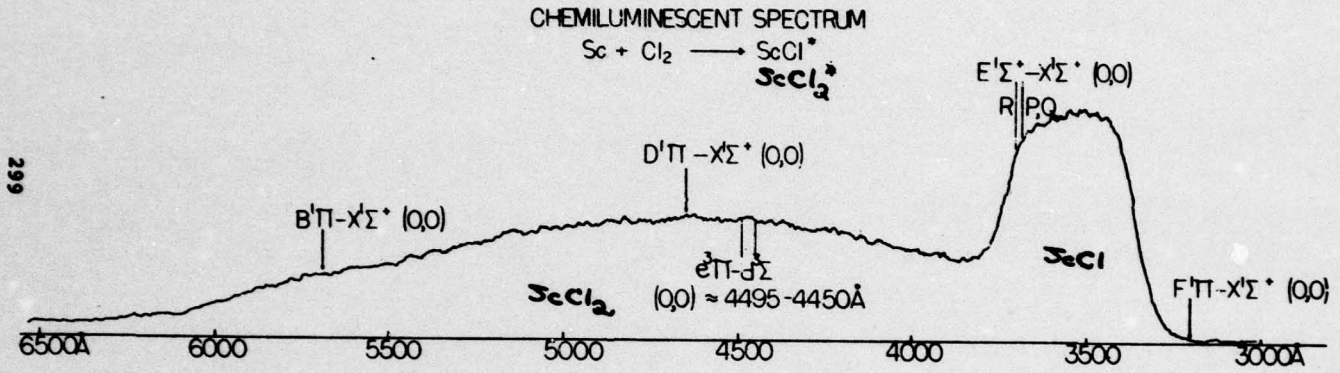
CHEMILUMINESCENT SPECTRUM
Sc + Cl2 ⟶ ScCl*
ScCl2*
E'Σ+ –X'Σ+ (0,0)
R P,Q
D'Π –X'Σ+ (0,0)
B'Π-X'Σ+ (0,0)
e³Π-d³Σ
(0,0) ≈ 4495-4450Å
ScCl
ScCl2
F'Π-X'Σ+ (0,0)
6500Å
6000
5500
5000
4500
4000
3500
3000Å

Figure 5

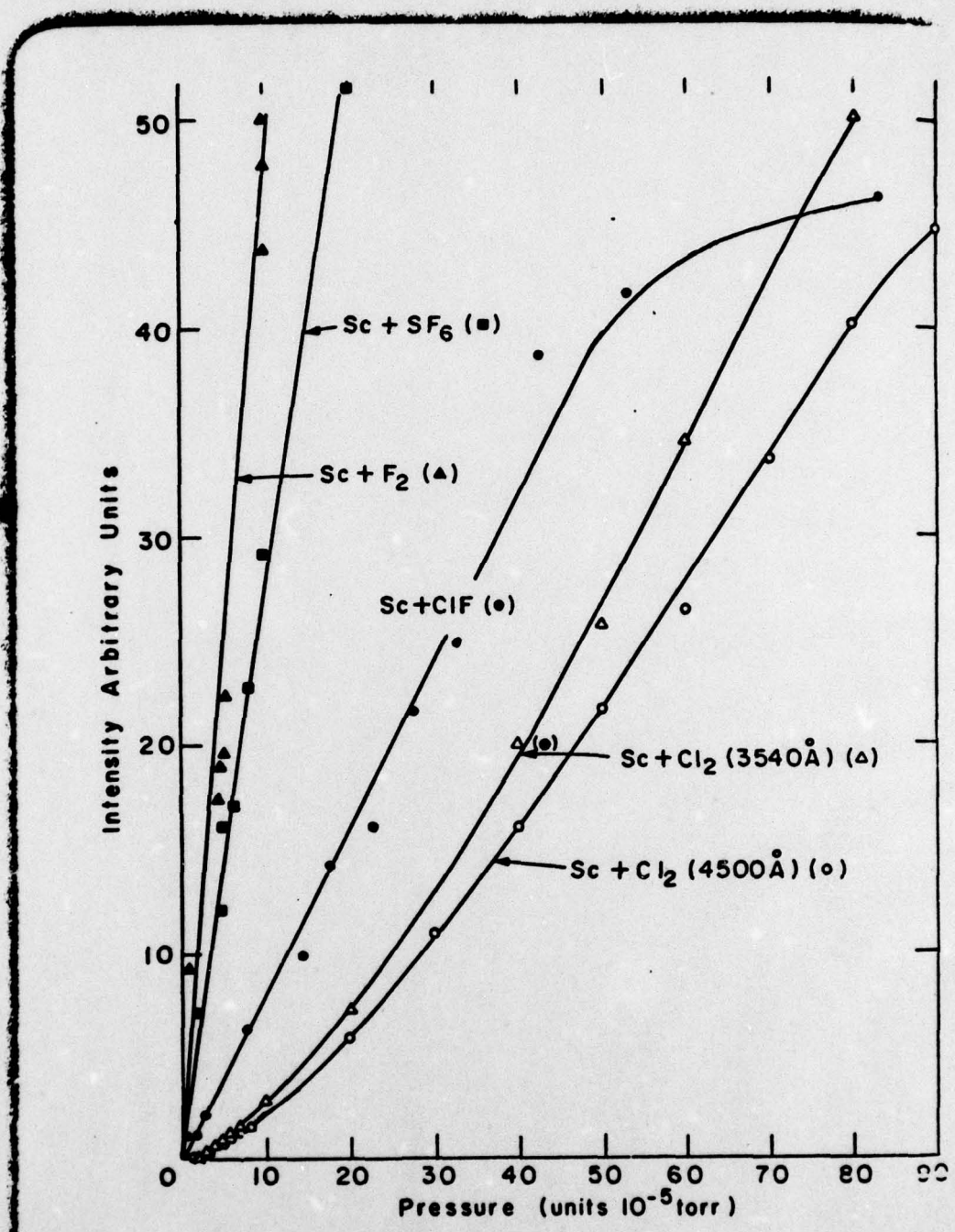
Intensity Arbitrary Units
Pressure (units 10^{-5} torr)
Sc + SF_6 (■)
Sc + F_2 (▲)
Sc+ClF (●)
Sc + Cl_2 (3540Å) (△)
Sc + Cl_2 (4500Å) (○)
0
10
20
30
40
50
60
70
80

Figure 6

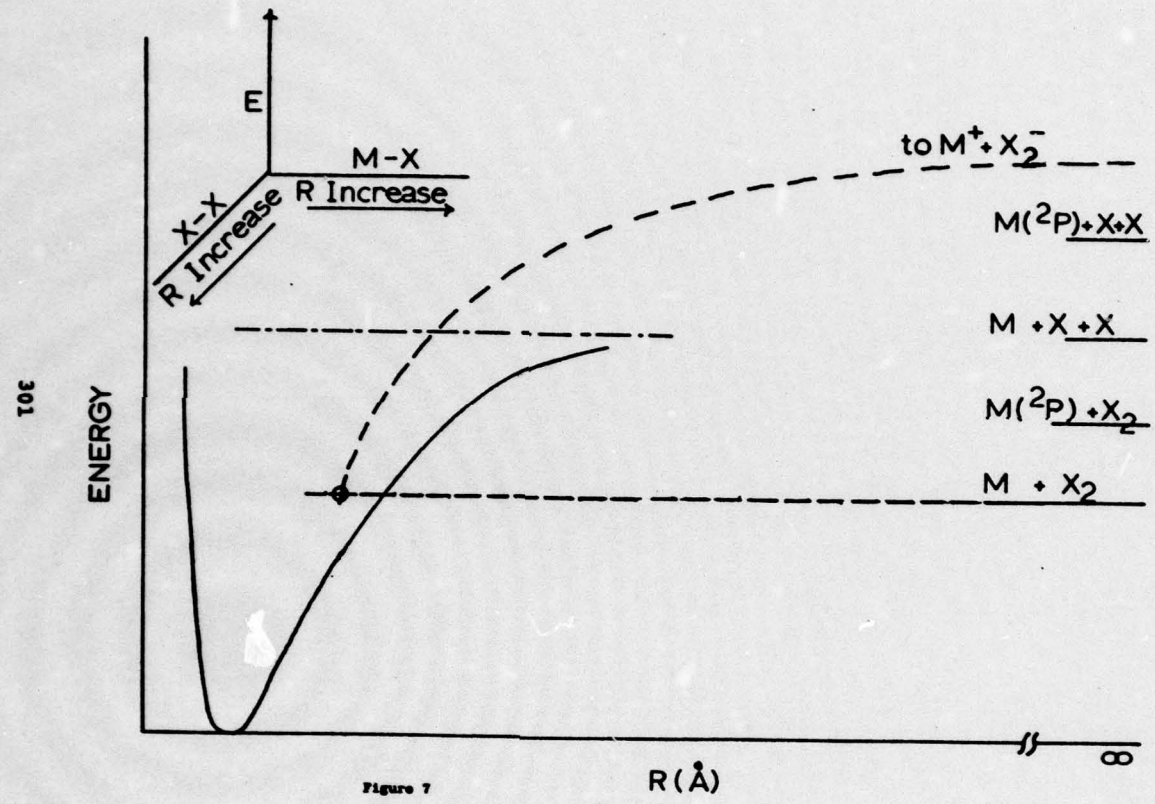
E
M-X
R Increase
X-X
R Increase
to $M^+ + X_2^-$
$M(^2P) + X + X$
$M + X + X$
$M(^2P) + X_2$
$M + X_2$
ENERGY
R(Å)
∞

Figure 7

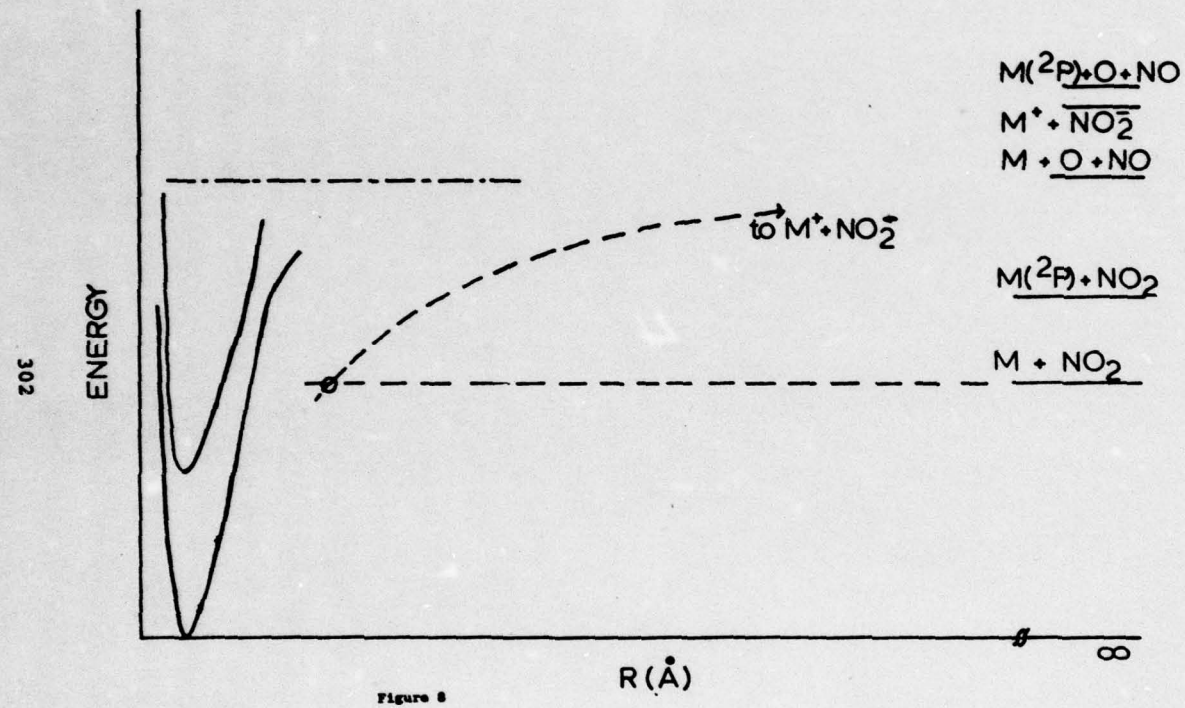

Figure 8

Table I

Group IIIB - Halogen Reactions Studied Product Formation

	Sc	Y	La
F_2	ScF^s	YF^s	LaF
Cl_2	$ScCl^s$, $ScCl_2{}^c$	YCl^s	LaCl
Br_2	$ScBr^s$, $ScBr_2{}^c$	YBr^s	---
I_2	ScI^s, $ScI_2{}^c$	YI^s	---
SF_6	ScF^s	YF^s	LaF
ClF	ScF^s	$YCl^s > YF^s$	LaF, LaCl
ICl	ScCl > ScI	$YCl^s > YI^s$	---
IBr	---	$YBr^s > YI^s$	---

s = selective monohalide emission

c = continuous emission due to dihalide

Table II

Observed and Estimated Electronic Energy Levels of ScF, TiO and ZrO

($cm^{-1} \times 10^{-3}$)

Molecular Orbital Configuration				Molecular State	ScF	TiO	ZrO
$s\sigma^2$				$^1\Sigma$	0.0	2.8	0.0
$s\sigma$	$d\delta$			$^3\Delta$	0.0	0.0	0.0
				$^1\Delta$	2.	0.6[a]	5.0
$s\sigma$		$d\pi$		$^3\Pi$	8	0	8
				$^1\Pi$	10.7[t]	11.9[t]	11
	$d\delta$	$d\pi$		$^3\phi$	15.3[t]	14.1[t]	16.7[t]
				$^3\Pi$	18.3[t]	16.2[t]	18.7[t]
				$^1\phi$	19	18.4[t]	20
				$^1\Pi$	20.3	19	21
$s\sigma$		$d\sigma$		$^3\Sigma$	14	13	14
				$^1\Sigma$	16.1[t]	15	16
	$d\delta$	$d\sigma$		$^3\Delta$	21.9[t]	19.3[t]	22.5[t]
				$^1\Delta$	24	22	24.3[t]
$s\sigma$			$p\pi$	$^3\Pi$	24	25	25
				$^1\Pi$	26.8[t]	22	27
	$d\delta$		$p\pi$	$^3\phi$	27.2[t]	25	27
				$^3\Pi$	31	29	31
				$^1\phi$	32	30	32
				$^1\Pi$	34.9[t]	33	35

t = experimentally identified states

Table III

Singlet States of YF

State	T_{00}	$G_{\frac{1}{2}}$	$x_e\omega_e$	B_0	$10^3 a$
$^1\Sigma$	31 205.8	536.3	2.13	0.27545	2.28
$^1\Pi$	27 989.9	547.5	2.69	0.2741	—
Π	26 046.4	--	--	0.2685	--
$^1\Pi$	25 464.5	--	--	0.2706	—
$^1\Pi$	25 324.9	--	--	0.2680	--
$C^1\Sigma$	19 190.3	527.2	2.45	0.2657	—
$B^1\Pi$	15 885.8	537.7	2.35	0.2657	1.56
$X^1\Sigma$	0	631.3	2.50	0.28960	1.63

Table IV

Quantum Yields for Electron Transfer Metal Oxidations

Reactions Studied	Quantum Yield (%)[a]
$Sc + F_2 \rightarrow ScF^* + F$	>5%
$Y + F_2 \rightarrow YF^* + F$	>9.1%[b]
$La + F_2 \rightarrow LaF^* + F$	>2.7%[b]
$Sc + NO_2 \rightarrow ScO^* + NO$	1.9%
$Y + NO_2 \rightarrow YO^* + NO$	10×10^{-2}%
$La + NO_2 \rightarrow LaO^* + NO$	$\approx 20 \times 10^{-2}$%[c]
$Ba + F_2 \rightarrow BaF^* + F$	$\approx 2.1 \times 10^{-3}$%[d]
$Ca + F_2 \rightarrow CaF^* + F$	3.8×10^{-3}%

[a] See references 3, 14, and 15.

[b] See text for discussion of radiative lifetimes and the proposed model for selectivity. The magnitude of these quantum yields is influenced by the long radiative lifetimes characterizing the emitters.

[c] Not including LaO $A'^2\Delta - X^2\Sigma^+$ emission; however, see ref. 31.

[d] Not including the BaF $A^2\Pi - X^2\Sigma^+$ system.

Table V

Activation Energies for Formation of ScO, YO, LaO

Reactions Studied	Activation Energy (kcals/mole)
$Sc + O_2 \rightarrow ScO^*(A^2\Pi_{1/2})$	5.13 ± 3.59
$Sc + NO_2 \rightarrow ScO^*(A^2\Pi_{1/2})$	7.85 ± 1.18
$Sc + NO_2 \rightarrow ScO^*(B^2\Sigma^+)$	6.43 ± 1.25
$Sc + N_2O \rightarrow ScO^*(A^2\Pi_{1/2})$	14.16 ± 2.44
$Y + O_2 \rightarrow YO^*(A^2\Pi_{3/2})$	1.75 ± 0.52
$Y + NO_2 \rightarrow YO^*(A^2\Pi_{3/2})$	1.10 ± 0.76
$Y + N_2O \rightarrow YO^*(A^2\Pi_{3/2})$	10.45 ± 1.23
$Y + O_2 \rightarrow YO^*(A'^2\Delta)$	≃0 ± 0.86
$La + O_2 \rightarrow LaO^*(C^2\Pi_{3/2})$	2.82 ± 1.59
$La + NO_2 \rightarrow LaO^*(C^2\Pi_{3/2})$	3.17 ± 1.78
$La + N_2O \rightarrow LaO^*(C^2\Pi_{3/2})$	2.81 ± 2.17

Table VI

Activation Energies for Excited State Metal Monohalide Formation

Reactions Studied[a]	Activation Energy (kcals/mole)
$Sc + F_2 \rightarrow ScF^*(^3\Sigma^+) + F$ (selective feature at 3460 Å)	0 ± 1.8
$Sc + Cl_2 \rightarrow ScCl^*(^3\Sigma^+) + Cl$ (selective feature at 3500 Å)	1.2 ± 1.5
$Y + F_2 \rightarrow YF^*(^3\Sigma^+) + F$ (selective feature at 3800 Å)	2.0 ± 8.1
$Y + F_2 \rightarrow YF^*(C^1\Sigma^+) + F$ (emission at 5000 Å)	12.8 ± 7.0
$Y + ClF \rightarrow YF^*(^3\Sigma^+) + Cl$ (selective feature at 3800 Å)	0 ± 3.1 0 ± 6.8
$Y + ClF \rightarrow YCl^*(^3\Sigma^+) + F$ (selective feature at 3900 Å)	3.9 ± 5.1 0 ± 2.7
$Y + IBr \rightarrow YBr^*(^3\Sigma^+) + I$ (selective feature at 4040 Å)	2.4 ± 1.6
$La + F_2 \rightarrow LaF^*(^1\Pi) + F$ (prominant feature at 4730 Å)	0.8 ± 1.6
$La + F_2 \rightarrow LaF^* + F$ (short wavelength feature at 4119 Å)	4.0 ± 2.1
$Ca + F_2 \rightarrow CaF^*(B^2\Sigma^+) + F$	3.7 ± 1.3
$Sr + F_2 \rightarrow SrF^*(B^2\Sigma^+) + F$	3.5 ± 0.8
$Sr + F_2 \rightarrow SrF^*(C^2\Pi^+) + F$	4.8 ± 1.0
$Sr + F_2 \rightarrow SrF^*(D^2\Sigma^+) + F$	4.0 ± 1.4

[a]See reference 16 and 19 for a discussion of activation energy determination in a beam-gas experiment.

Table VII

Dissociation Energies - Group IIIB Monohalides

Reaction	Product	$E_{int}(MX)$ (cm^{-1})	$E_{int}(M)$ (cm^{-1})	$E_{int}(RX)$ (cm^{-1})	E_T^i (cm^{-1})	$D_0^0(MX)$ (eV) Lower Bound	Literature[a] (eV)
Sc + F_2	ScF	31726	96	221	1172	5.36 ± 0.10	6.06 ± 0.14
Sc + ClF	ScF*	21746	96	226	1342	6.34 ± 0.10	6.06 ± 0.14
Sc + SF_6	ScF	31746	96	914	1668	(7.07 ± 0.10)[b]	6.06 ± 0.14
Sc + Cl_2	ScCl	31516	96	249	1461	6.16 ± 0.10	----------
Sc + Br_2	ScBr	31260	96	296	1777	5.58 ± 0.10	----------
Y + F_2	YF	38506	271	221	870	6.21 ± 0.10	6.18 ± 0.22
Y + ClF	YF	30211	268	227	981	6.18 ± 0.10	6.18 ± 0.22
Y + SF_6	YF	28571	268	914	1409	6.69 ± 0.10	6.18 ± 0.22
Y + Cl_2	YCl	26918	268	249	1094	5.62 ± 0.10	----------
Y + Br_2	YBr	27568	268	296	1514	5.01 ± 0.10	----------
La + F_2	LaF	32144	448	221	738	5.42 ± 0.10	----------
La + ClF	LaF	29525	453	227	856	6.08 ± 0.10	----------
La + SF_6	LaF	29369	453	914	1328	6.78 ± 0.10	----------
La + Cl_2	LaCl	29369	453	249	983	5.92 ± 0.10	----------

[a]See reference 27.

[b]This is a tentative value.